L-358

ARR No. 3J23

NATIONAL ADVISORY COMMITTEE FOR AERONAUTICS

WARTIME REPORT

ORIGINALLY ISSUED
October 1943 as
Advance Restricted Report 3J23

EFFECT OF LENGTH-BEAM RATIO ON RESISTANCE AND SPRAY OF THREE MODELS OF FLYING-BOAT HULLS

By Joe W. Bell, Charlie C. Garrison, and Howard Zeck

Langley Memorial Aeronautical Laboratory
Langley Field, Va.

NACA

WASHINGTON

NATIONAL ADVISORY COMMITTEE FOR AERONAUTICS

ADVANCE RESTRICTED REPORT

EFFECT OF LENGTH-BEAM RATIO ON RESISTANCE AND SPRAY OF THREE MODELS OF FLYING-BOAT HULLS

By Joe W. Bell, Charlie C. Garrison, and Howard Zeck

SUMMARY

An investigation of the effect of changes in the length-beam ratio of flying-boat hulls on resistance and spray was conducted in NACA tank no. 1. A family of three models of hulls of different length-beam ratios was used and, in order to maintain comparable hull sizes, the plan-form areas of the hulls were made approximately equal by keeping equal products of length and beam.

The tests were made by the general method for the fixed-trim condition as well as by the specific method for the free-to-trim condition. Photographs of the spray were taken during the free-to-trim tests. Resistance and trimming-moment data obtained from the tests were compared over a wide range of loads at best-trim and free-to-trim conditions. Further comparisons were made by means of take-off calculations for hypothetical flying boats that incorporated the lines of the models.

The spray photographs indicated that at very low speeds the height of the bow spray was reduced by increasing the length-beam ratio, but at high speeds the height of the spray was increased slightly by increasing the length-beam ratio. It was concluded from the results of the tests that by increasing the length-beam ratio the load coefficient may be increased and that, within the range of the tests, high length-beam ratios will give lower hump resistance and better take-off performance than low length-beam ratios.

INTRODUCTION

The trend in the design of modern flying boats to decrease the frontal area by decreasing the beam increases the beam loading and requires an increase in length-beam

ratio L/b to maintain suitable hydrodynamic characteristics. The available information on the effect of changes in the length-beam ratio is contained in references 1, 2, and 3. The analysis of this information is mainly concerned with increase in length for a given beam, which causes the effect of increase in size of the hull to obscure the effect of length-beam ratio.

The present investigation was undertaken to determine the effect of changing the length-beam ratio and of keeping the size of the hull constant at the same time - that is, the effect of changing the proportions of the hull for a given flying boat without changing the volume. The proportions for such a series could not be determined exactly without detail designs for each hull but have been approximated by maintaining a constant value of the product of lenth and beam for the models with different length-beam ratios.

Three models of flying-boat hulls with a variation in length-beam ratio of 50 percent were used in the investigation. The range of length-beam ratios tested covered the range used on modern flying boats. The models were tested over a wide range of loadings in order to include the effect of changes in load coefficient.

DESCRIPTION OF MODELS

Photographs of the three models tested are shown in figures 1 and 2. These models are designated NACA models 144, 145, and 146. Typical sections are shown in figure 3, and the offsets used in the construction of the models are given in tables I, II, and III.

The parent form of the series, NACA model 144, was identical with NACA model 84-AF (reference 4) except for an increase in the depth of step. After the models had been constructed, this depth was increased from 0.4 inch to 1.0 inch for all the models, or from 2.5 percent to 6.28 percent of the beam of the parent form. This increase in the depth of step was made because tests of dynamic models of flying boats have indicated that skipping and high-angle porpoising might result from the use of the original depth of step.

When the forms of NACA models 145 and 146 were derived, the product of length and beam of each model was

made equal to that of model 144, and the corresponding transverse sections of the bottom surfaces were made geometrically similar. Other values made the same for the three models were: angle of dead rise, angle of forebody keel, angle of afterbody keel, height of hull, and depth of step.

The following equations give the relationship of the dimensions of the derived models to those of the parent model:

$$L_d b_d = L_p b_p$$

$$\frac{L_d}{b_d} = K \frac{L_p}{b_p}$$

$$L_d = \sqrt{K}\, L_p$$

$$b_d = \frac{1}{\sqrt{K}}\, b_p$$

$$h_d = \frac{1}{\sqrt{K}}\, h_p$$ (except for corrections applied to maintain equal angles of keel, equal depth of step, and equal over-all height)

where

L_d any longitudinal dimension of derived model

L_p longitudinal dimension of parent model corresponding to L_d

b_d any transverse dimension of derived model

b_p transverse dimension of parent model corresponding to b_d

h_d any vertical dimension of derived model

h_p vertical dimension of parent model corresponding to h_d

K constant (1.25 for model 145 and 1.50 for model 146)

In order to maintain the same angles of the keel, a correction was applied that corresponded to the vertical

change resulting from moving the section longitudinally parallel to the straight portion of the keel. In order to make the depth of step equal to that of the parent model, the entire afterbody was moved vertically by a constant amount. The bow of the derived model was brought to the same height as the bow of the parent model by arbitrarily raising the sections forward of station 2. The deck was located at the same height as the deck of the parent model. The curved portions of the deck line at the bow and the stern were made identical with the curved portions of the deck line of the parent model, and the length of the straight portion was extended by the full amount of the increase in length of the model.

The following table summarizes the principal dimensions of the models:

	NACA model 144	NACA model 145	NACA model 146
Over-all length, inches	114.85	128.41	140.67
Length to stern post, inches	83.33	93.17	102.06
Length of forebody, inches	50.10	56.02	61.36
Length of afterbody, inches	33.23	37.15	40.70
Maximum beam, inches	15.92	14.24	13.00
Length-beam ratio	5.23	6.54	7.84
Length-beam product, square inches	1327	1327	1327
Angle of dead rise, degrees	20	20	20
Angle of afterbody keel, degrees	5.5	5.5	5.5
Angle of forebody keel, degrees	1.3	1.3	1.3
Depth of step, inches	1.0	1.0	1.0
Depth of step, percent beam	6.28	7.02	7.70
Center of gravity, forward of step, inches	7.2	7.2	7.2
Center of gravity, height above keel line at step, inches	17.94	17.94	17.94

The models were constructed of laminated mahogany and were built in two sections that joined at the step. They were finished with pigmented varnish.

APPARATUS AND METHODS

The models were tested in NACA tank no. 1 by the use of the standard equipment and methods described in reference 5. The water in the tank was at the 12-foot level

during the tests. Both the specific free-to-trim method and the general fixed-trim method were used. The assumed center of gravity, located 7.20 inches forward of the step and 17.94 inches above the keel, was taken as the pivot for the free-to-trim tests and as the center of trimming moments for the general tests.

In the free-to-trim tests, the hydrofoil lift device was used to simulate the lift of a hypothetical wing. The lift was applied at the center of gravity, and the same wing was assumed for each of the models. The load schedule for the general tests was chosen to include all loads and speeds of interest for preliminary design, and a sufficient number of trims were used to determine the data at best trim and at zero trimming moment. Three typical loads in the range of the general schedule were assumed for the free-to-trim tests.

RESULTS

The usual tares, as described in reference 5, were applied to the data collected from the tests. The corrected data were plotted in dimensional form because the beams of the models were not equal. This method of plotting permits a more direct comparison of the characteristics. A few of the plots were made, however, using nondimensional coefficients in order to compare the models on the basis of equal beam. The coefficients used are defined as follows:

C_{Δ} load coefficient $\left(\frac{\Delta}{wb^3}\right)$

C_{Δ_o} initial load coefficient $\left(\frac{\Delta_o}{wb^3}\right)$

C_V speed coefficient $\left(\frac{V}{\sqrt{gb}}\right)$

where

Δ load on water, pounds

Δ_o initial load on water, pounds

w specific weight of water, pounds per cubic foot (63.5 lb/cu ft for NACA tank no. 1)

b beam of hull, feet

g acceleration of gravity, feet per second per second (32.2 ft/sec^2)

V speed, feet per second

The data obtained in the general tests are presented as curves of resistance and trimming moment plotted against speed at various trims and loads in figures 4 to 9 for model 144, in figures 10 to 16 for model 145, and in figures 17 to 23 for model 146.

For the determination of the best trim and the resistance at best trim, the data from the original resistance curves were cross-plotted against trim. From these plots, best trim, resistance at best trim, and trimming moment at best trim were determined, and each was plotted against speed in figures 24 to 26.

For the free-to-trim tests, resistance and trim were plotted atainst speed in figures 27 to 29. From the curves of resistance and load on the water, the values of load-resistance ratio Δ/R were obtained and plotted on the same sheets. Get-away speed V_G was computed for each initial load. Figure 30 shows the load curves for the specific tests at various initial loads for all the models in terms of load coefficient and speed coefficient.

DISCUSSION

Resistance.- Comparison of the resistance curves from the fixed-trim tests of the three models (figs. 4 to 23) shows that increasing the length-beam ratio resulted in a decrease in the resistance at hump speeds and at low speeds and an increase in the speed at which the hump occurred. These trends held true for all trims that were investigated.

A comparison of the effect of different length-beam ratios on resistance at best trim for the three models is given in figure 31. In general, the same conclusions drawn from comparisons of resistance at equal trims hold

for resistance at best trim. At low speeds, an increase in the value of length-beam ratio reduced the resistance at best trim. The hump occurred at successively higher speeds, going from low values to high values of length-beam ratio. The maximum resistance at the hump was reduced about 7 percent by changing the length-beam ratio from 5.23 to 6.54, but was not changed appreciably when the length-beam ratio was increased from 6.54 to 7.84. At high speeds and intermediate loads (speeds above 30 fps and loads of 40 to 80 lb, model size), the resistance was reduced as the length-beam ratio was increased. At high speeds and light loads, no significant effect resulted from changing the length-beam ratio.

Curves of trim and resistance at zero trimming moment for each of the models at an initial load of 100 pounds are combined for comparison in figure 32. The effects in the free-to-trim condition were substantially the same as those found at equal fixed trims and at best trim. Increasing the length-beam ratio caused a reduction in resistance at low speeds and at the hump and caused the hump to occur at a higher speed.

Curves of the variation of load-resistance ratio Δ/R with load for models 144, 145, and 146 are shown in figure 33(a). The data in these curves were taken directly from the curves of resistance (best trim and free to trim) of the models. Comparison of these curves shows the effects of changing length-beam ratio without causing a significant change in the volume of the hull or the area of the plan form. These curves show that in both the best-trim and the free-to-trim conditions Δ/R was made larger by increasing the length-beam ratio from 5.23 to 6.54 but was not changed appreciably by a further increase to a length-beam ratio of 7.84. The curves of Δ/R at best trim show that, at a speed of 40 feet per second, increasing the length-beam ratio increased Δ/R at the heavier loads but had no significant effect at loads below 25 pounds.

The curves in figure 33(b) were derived by converting the data from models 144 and 146 to values for two hypothetical models having the lines of models 144 and 146 and lengths equal to the length of model 145. Comparison of these curves shows that, within the range included in the tests, increasing the beam without changing the length would increase Δ/R at the hump. This effect is present in both the free-to-trim and the best-trim condi-

tions and at all loads included in the investigation. Comparison of the curves representing a speed of 40 feet per second shows that in the high-speed condition Δ/R would be decreased by increasing the beam.

Curves of variation of load-resistance ratio Δ/R with load coefficient C_Δ are shown in figure 34. Inasmuch as the coefficients used incorporate the beam as the characteristic dimension, comparisons made in terms of these coefficients show the same relative values as would be shown in comparisons of data for models of equal beam and different lengths. In general, this comparison indicates that, within the range of length-beam ratios investigated, increasing the length of a hull would improve Δ/R at the hump but would cause lower values of Δ/R at speeds near get-away. At best trim, the data indicate that increasing the length-beam ratio from 5.23 to 6.54 (by lengthening the hull) would cause a relatively large increase in Δ/R at the hump and that a further increase to a value of 7.84 would increase Δ/R by a lesser amount. In the free-to-trim condition, an increase from a length-beam ratio of 5.23 to 6.54 would increase Δ/R at the hump, but a further increase to a value of 7.84 would make no significant change in Δ/R at the hump. It is believed that these trends would hold true for hulls operating at the conditions of the test but, because of the dependence upon the location of the center of gravity, the trends indicated by the free-to-trim data might not apply in other cases.

A comparison of the curves of figure 34(a) shows that increasing the length of a hull similar to model 144 (without changing the beam) would result in a reduction of Δ/R at speeds near get-away. This trend appears to remain constant throughout the range of length-beam ratio from 5.23 to 7.84 and, inasmuch as increasing the length of the forebody cannot be expected to change the wetted area when the hull is planing at high speed, the increase in resistance may be attributed to the increased length of the afterbody.

The effects of changing length and beam on resistance may be summarized as follows: Increasing beam alone or length alone increases Δ/R at the hump speed and decreases Δ/R at high planing speeds; increasing length-beam ratio without changing the plan-form area increases Δ/R at the hump and causes little change in Δ/R at high planing speeds.

Spray.- Photographs of the spray formations of the three models are shown in figures 35 and 36. These photographs were taken during the specific tests in the free-to-trim condition. The models were compared at equal initial loads and equal speeds; however, the load coefficients for the models differed by as much as 85 percent. At low speeds, the short models (with small length-beam ratios) produced higher bow spray than the long models; near the hump speeds and planing speeds, the spray was a little higher for the models with narrow beams. (See figs. 35 and 36.)

When the length and the beam were the only variables in hull dimensions, as in figures 35 and 36, there appeared to be an indication that the spray was more dependent upon the area of the planing surfaces than upon the beam itself. For this reason, the load coefficient should not be taken as a definite criterion for the loading of a hull unless the length-beam ratio also is considered.

Take-off performance.- In order to compare the overall resistance of the models, take-off calculations were made for a series of load coefficients. Hypothetical flying boats were assumed, with models 144, 145, and 146 used as the hulls. The hulls of these flying boats were assumed to be 10.5, 11, and 12 times the size of the model hulls. The characteristics, which are the same for all the flying boats, are as follows:

Gross load, pounds	140,000
Wing area, square feet	3,500
Total horsepower at take-off (four engines)	9,200
Engine speed, revolutions per minute	2,600
Gear reduction	16:5
Propeller:	
Diameter, feet	19.3
Number of blades	3
Flaps:	
Type	Split
Span, percent wing span	60.0
Chord, percent wing chord	20.0
Aspect ratio	10
Effective aspect ratio, including ground effect	20
Parasite-drag coefficient (excluding hull)	0.02
Wing loading, pounds per square foot	40
Power loading, pounds per horsepower	15.2
Stalling speed, feet per second	132
Get-away speed, feet per second	145

The lift and drag curves of the wing, which were corrected for ground effect for use in the calculations, were taken from reference 6. The deflection of the flaps was taken as 30°.

In order to make several take-off plots, a series of three load coefficients was used for each model for a given gross weight. (See figs. 37 to 39.) The load coefficients used covered the entire range of the tests. The free-to-trim condition was used up to and slightly beyond the hump to 45 percent of get-away speed. Above this speed, precision trim (trim for minimum total resistance) was used. The method used for the calculations of take-off time and distance is described in reference 5.

The trend of the curves of total resistance (resistance plus drag, R + D) followed the trend of the resistance curves from the fixed-trim tests. At high planing speeds, the spray on the afterbodies caused the resistance to increase with longer afterbodies. The effect of the length-beam ratio on resistance was not critical at the speeds near get-away.

In every case the larger length-beam ratio gave better take-off performance. The length-beam ratio that would give the shortest take-off time and distance was not determined because it was beyond the scope of the length-beam ratios used in the tests. The limit of the length-beam ratio of a flying boat, however, may not be determined by resistance alone but by such other factors as aerodynamic and hydrodynamic stability, structural considerations, and usable space inside the hull.

CONCLUSIONS

As a result of this investigation, it is concluded that increasing the length-beam ratio within the range of 5.33 to 7.84 without changing the length-beam product causes the following changes in the characteristics of a flying-boat hull:

1. Higher hump speed and lower hump resistance

2. Lower bow spray at low speeds and slightly higher spray at high speeds (When the length and beam are the only variables, spray characteristics are more dependent

upon the length–beam product than upon the beam alone.)

3. Better take–off performance

4. Higher permissible load coefficients

Langley Memorial Aeronautical Laboratory,
National Advisory Committee for Aeronautics,
Langley Field, Va.

REFERENCES

1. Shoemaker, James M., and Parkinson, John B.: Tank Tests of a Family of Flying–Boat Hulls. T. N. No. 491, NACA, 1934.

2. Sottorf, W.: The Design of Floats. T.M. No. 860, NACA, 1938.

3. Davidson, Kenneth S. M., and Locke, F. W. S., Jr.: Some Systematic Model Experiments on the Porpoising Characteristics of Flying–Boat Hulls. NACA A.R.R. No. 3F12, June 1943.

4. Parkinson, John B., Olson, Roland E., Draley, Eugene C., and Luoma, Arva A.: Aerodynamic and Hydrodynamic Tests of a Family of Models of Flying–Boat Hulls Derived from a Streamline Body – NACA Model 84 Series. NACA A.R.R. No. 3I15, Sept. 1943.

5. Truscott, Starr: The Enlarged N.A.C.A. Tank, and Some of Its Work. T.M. No. 918, NACA, 1939.

6. Olson, R. E., and Allison, J. M.: The Calculated Effect of Various Hydrodynamic and Aerodynamic Factors on the Take–Off of a Large Flying Boat. Rep. No. 702, NACA, 1940.

TABLE I. - OFFSETS OF MODEL 144, INCHES

Station	Distance from F.P.	D	R	a	b	c	d	e	f	g	r
1	0.60		1.24	1.33	0.88			0.97	0.99	0.92	0.73
2	2.85		3.04	3.25	3.14			2.36	2.43	2.26	1.78
3	5.10		4.16	4.45	2.92			3.23	3.33	3.08	2.44
4	9.60		5.67	6.04	3.98			4.38	4.54	4.18	3.32
5	14.10		6.63	7.07	4.65			5.13	5.30	4.90	3.88
6	18.60		7.22	7.70	5.07			5.59	5.78	5.34	4.22
7	23.10		7.61	8.10	5.33			5.89	6.09	5.62	4.45
8	27.60		7.81	8.32	5.47			6.05	6.25	5.77	4.57
9	32.10		7.93	8.47	5.56			6.14	6.34	5.86	4.64
10	36.60		7.96	8.58	5.66			6.25	6.37	5.97	4.66
11	41.10	0.02	7.94	8.68	5.76			6.35	↑	6.07	↑
12	45.60	.09	7.87	8.78	5.89			6.45	|	6.17	|
13F	50.10	.21	7.75	8.88	6.04			6.55	|	6.27	|
13A				7.88	5.04			5.55	6.37	5.87	|
14	54.60	.98	7.58	7.45	4.69	0.19	7.52	5.20	6.14	4.92	|
15	59.10	1.19	7.37	7.02	4.40	.29	7.14	4.91	5.76	4.63	|
16	63.60	1.45	7.11	6.58	4.19	.42	6.53	4.70	5.15	4.42	|
17	68.10	1.76	6.80	6.15	4.08	.58	5.65	4.59	4.27	4.31	|
18	72.60	2.11	6.45	5.72	4.08	.75	4.49	4.59	3.11	4.31	|
19	77.10	2.51	6.05	5.28	4.20	.92	2.96	4.71	1.58	4.43	|
20	81.60	2.95	5.61	4.85	4.48	1.42	1.02	4.85		4.57	|
21	83.33	3.13	5.43	4.68	4.68	1.88				4.68	4.66
22	86.10	3.44	5.12								
23	90.60	3.97	4.59								
24	95.10	4.55	4.01								
25	99.60	5.17	3.39								
26	104.10	5.83	2.73								
27	108.60	6.53	2.03								
28	112.80	7.24	1.23								
29	114.00	7.47	.87								
30	114.60	7.58	.51								
A.P.	114.85	7.64									

TABLE II. - OFFSETS OF MODEL 145, INCHES

Station	Distance from F.P.	D_1	D_2	R	a	b	c	d	e	f	g	r
F.P.		0.25	0.94		-0.96	-0.96			-0.96		-0.96	
1	0.67	.25	1.18	1.11	.85	.39			.49	0.89	.45	0.65
2	3.19	.24	1.46	2.72	2.68	1.68			1.89	2.17	1.80	1.59
3	5.70	.23	1.65	3.72	3.76	2.38			2.66	2.98	2.52	2.18
4	10.73	.21	1.84	5.07	5.21	3.35			3.71	4.06	3.53	2.97
5	15.77	.18	1.89	5.93	6.14	3.98			4.41	4.74	4.20	3.47
6	20.80	.16	1.89	6.50	6.73	4.37			4.84	5.17	4.62	3.77
7	25.83	.13	1.89	6.81	7.11	4.63			5.13	5.45	4.89	3.98
8	30.86	.11	1.85	6.99	7.33	4.78			5.29	5.59	5.04	4.09
9	35.89	.09	1.80	7.09	7.49	4.88			5.40	5.67	5.15	4.15
9A	36.60		1.80	7.10								
10	40.92	.07	1.78	7.12	7.60	4.99			5.52	5.70	5.27	4.17
11	45.95	.06	1.80	7.10	7.72	5.11			5.63	↑	5.38	↑
12	50.99	.11	1.86	7.04	7.83	5.24			5.74	↕	5.49	↕
13F	56.02	.22	1.97	6.93	7.94	5.40			5.86	↕	5.61	↕
13A					6.94	4.49			4.86	5.70	4.61	↕
14	61.05	1.04	2.72	6.78	6.46	3.99	0.13	6.73	4.45	5.49	4.30	↕
15	66.08	1.32	2.91	6.59	5.98	3.64	.22	6.39	4.09	5.15	3.84	↕
16	71.11	1.65	3.14	6.36	5.49	3.35	.34	5.84	3.81	4.61	3.55	↕
17	76.14	2.02	3.42	6.08	5.01	3.16	.48	5.05	3.62	3.82	3.37	↕
18	81.17	2.43	3.73	5.77	4.53	3.06	.63	4.02	3.52	2.78	3.27	↕
19	86.21	2.89	4.09	5.41	4.04	3.07	.76	2.65	3.53	1.42	3.28	↕
20	91.24	3.38	4.48	5.02	3.55	3.22	1.23	.91	3.55		3.30	4.17
21	93.17	3.58	4.64	4.86	3.37	3.37	1.64	.18 rad			3.37	
22	96.27	3.92	4.92	4.58								
23	101.30	4.49	5.39	4.11								
24	106.33	5.10	5.91	3.59								
25	111.36	5.75	6.47	3.03								
26	116.39	6.44	7.06	2.44								
27	121.43	7.18	7.68	1.82								
27A	122.16	7.29	7.78	1.72								
28	126.12	7.99	8.31	1.10								
29	127.46	8.29	8.52	.78								
30	128.13	8.48	8.62	.46								
A.P	128.41	8.58	8.58									

TABLE III. - OFFSETS OF MODEL 146, INCHES

Station	Distance from F.P.	D_1	D_2	R	a	b	c	d	e	f	g	r
F.P.		0.47	1.63		-1.63	-1.63			-1.63		-1.63	
1	0.73	.46	2.02	1.01	.24	-.15			-.07	0.81	-.10	0.60
2	3.49	.44	2.58	2.48	2.21	1.31			1.49	1.98	1.40	1.45
3	6.25	.42	2.86	3.40	3.22	1.97			2.22	2.72	2.10	1.99
4	11.76	.38	3.18	4.67	4.56	2.91			3.20	3.71	3.04	2.71
5	17.27	.33	3.32	5.42	5.44	3.48			3.85	4.33	3.67	3.17
6	22.78	.29	3.34	5.90	5.99	3.85			4.27	4.72	4.07	3.45
7	28.29	.25	3.28	6.21	6.36	4.10			4.56	4.97	4.34	3.63
8	33.80	.21	3.22	6.38	6.58	4.25			4.73	5.10	4.50	3.73
8A	36.60		3.18	6.43								
9	39.32	.16	3.17	6.47	6.75	4.38			4.85	5.18	4.62	3.79
10	44.83	.12	3.12	6.50	6.88	4.50			4.98	5.20	4.75	3.80
11	50.34	.10	3.13	6.48	7.01	4.62			5.10	↑	4.87	↓
12	55.85	.11	3.19	6.43	7.13	4.71			5.23	↓	5.00	↓
13F	61.36	.26	3.29	6.33	7.25	4.93			5.35	↓	5.12	↓
13A					6.25	3.94			4.35	5.20	4.12	↓
14	66.87	1.09	4.02	6.19	5.72	3.47	0.08	6.14	3.89	5.01	3.66	↓
15	72.39	1.43	4.19	6.02	5.20	3.03	.17	5.83	3.48	4.70	3.25	↓
16	77.90	1.82	4.40	5.81	4.66	2.71	.27	5.33	3.13	4.20	2.90	↓
17	83.41	2.26	4.65	5.57	4.13	2.44	.40	4.61	2.86	3.49	2.63	↓
18	88.92	2.71	4.94	5.27	3.61	2.28	.54	3.67	2.69	2.54	2.47	↓
19	94.43	3.22	5.28	4.94	3.07	2.21	.66	2.42	2.60	1.36	2.38	↓
20	99.94	3.74	5.63	4.58	2.54	2.24	1.09	.83	2.54		2.31	3.80
21	102.06	3.97	5.79	4.43	2.33	2.33	1.47	.16 rad			2.33	
22	105.46	4.33	6.03	4.18								
23	110.97	4.93	6.48	3.74								
24	116.48	5.58	6.94	3.28								
25	121.99	6.22	7.43	2.77								
26	127.50	6.92	7.98	2.23								
27	133.01	7.72	8.58	1.64								
27A	134.42	7.98	8.72	1.48								
28	138.16	8.57	9.13	1.00								
29	139.63	8.87	9.30	.71								
30	140.36	9.10	9.35	.42								
A.P.	140.67	9.27	9.27									

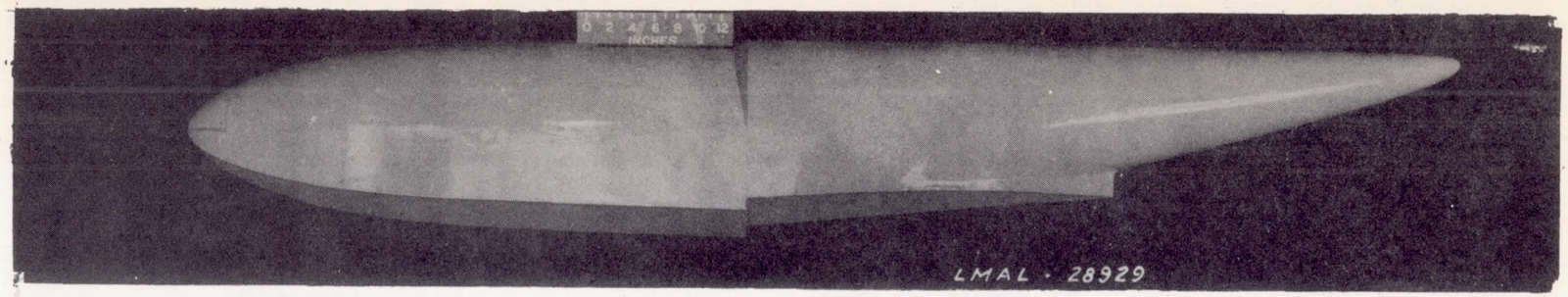

Model 144

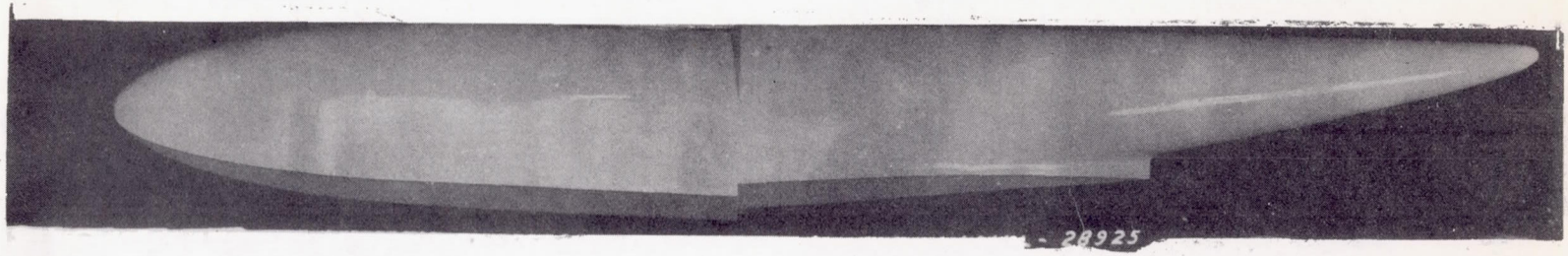

Model 145

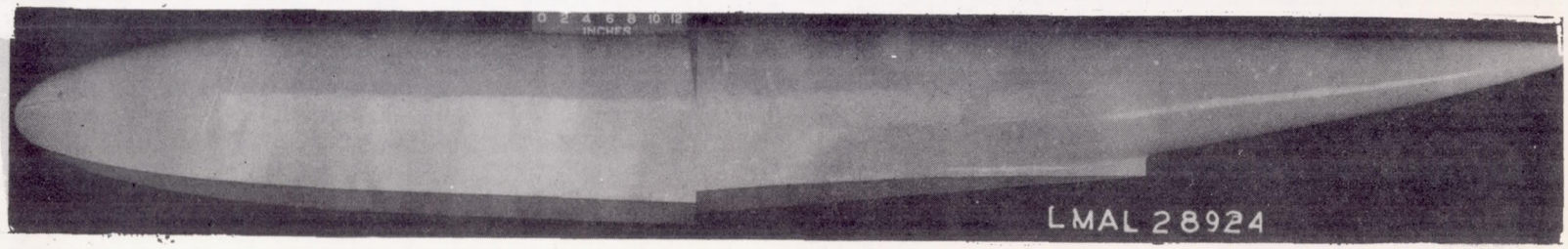

Model 146

Figure 1.- Profile views of NACA models 144, 145, and 146.

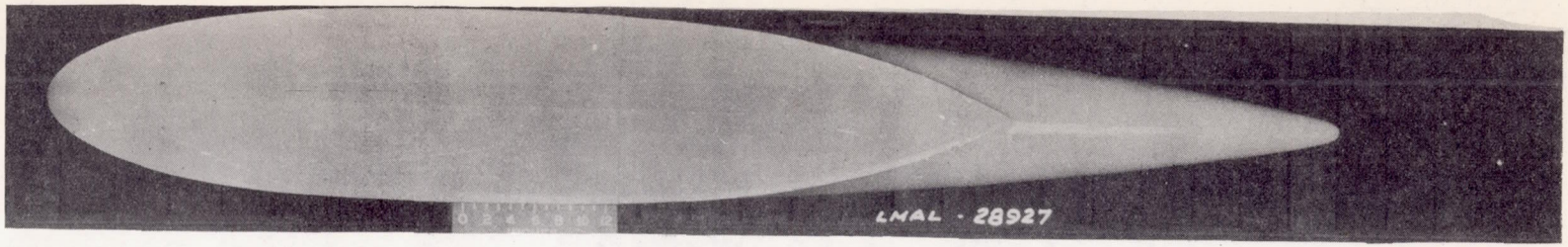

Model 144

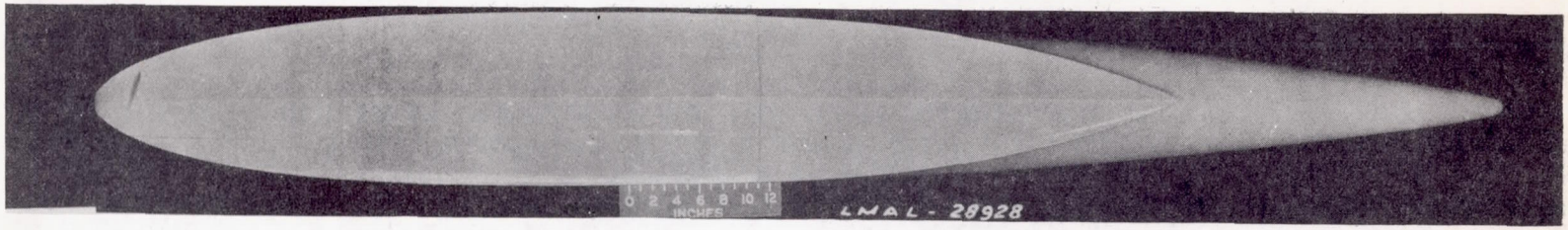

Model 145

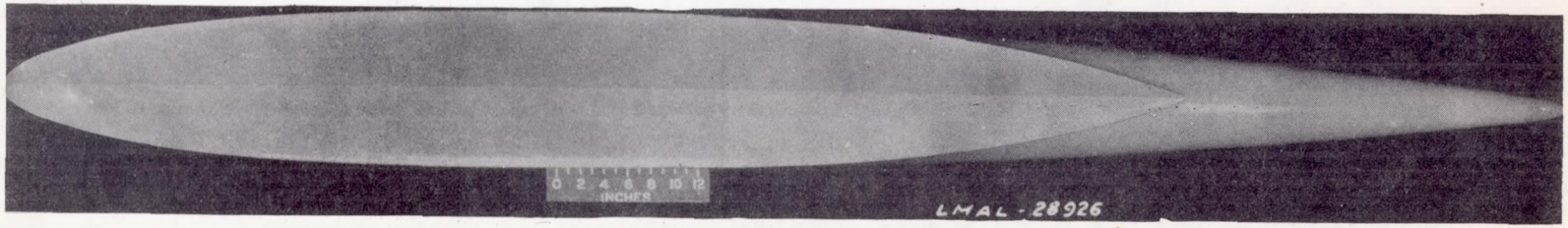

Model 146

Figure 2.- Plan-form views of NACA models 144, 145, and 146.

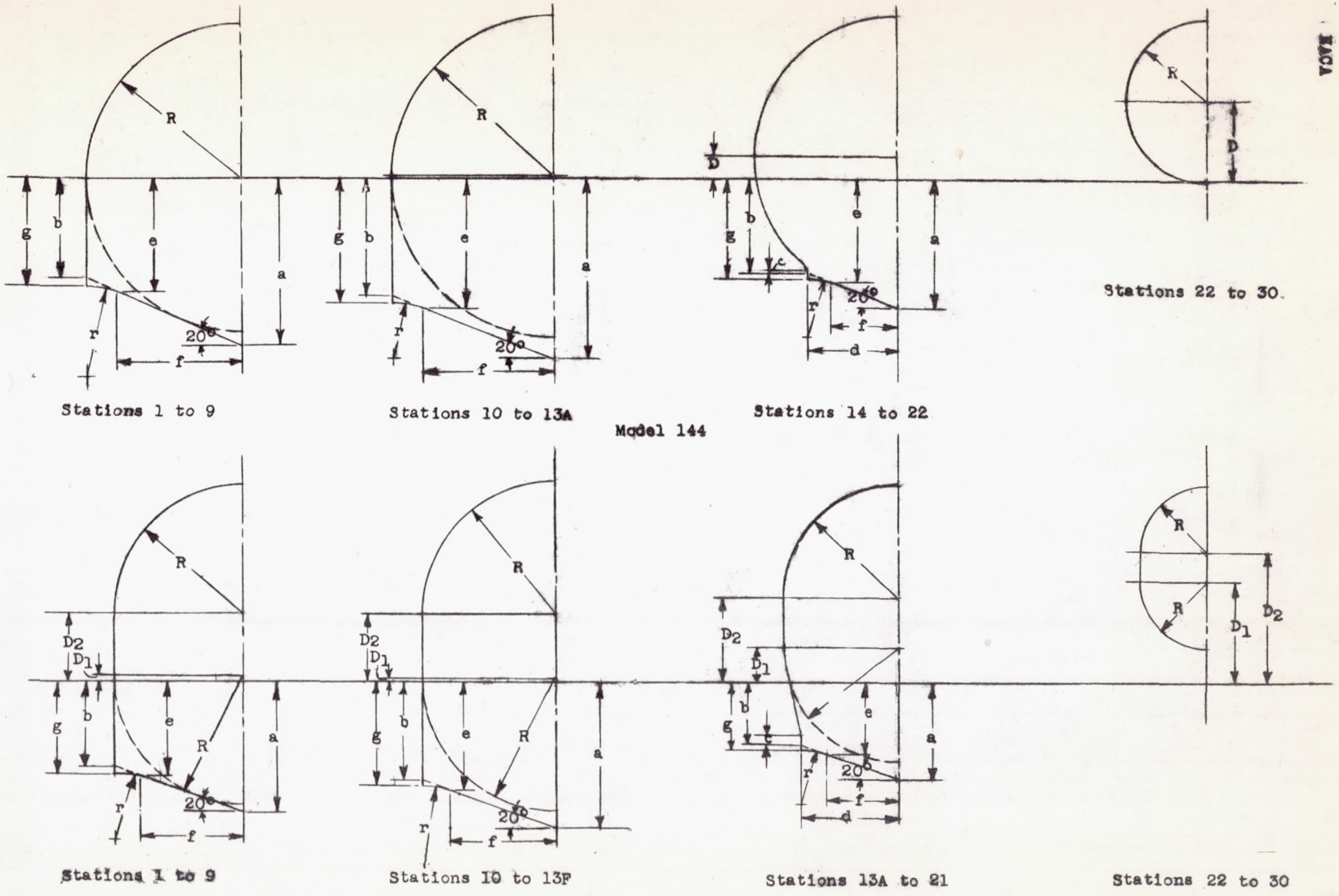

Figure 3.- Typical sections of models 144, 145, and 146, and definitions of symbols used in tables I, II, and III.

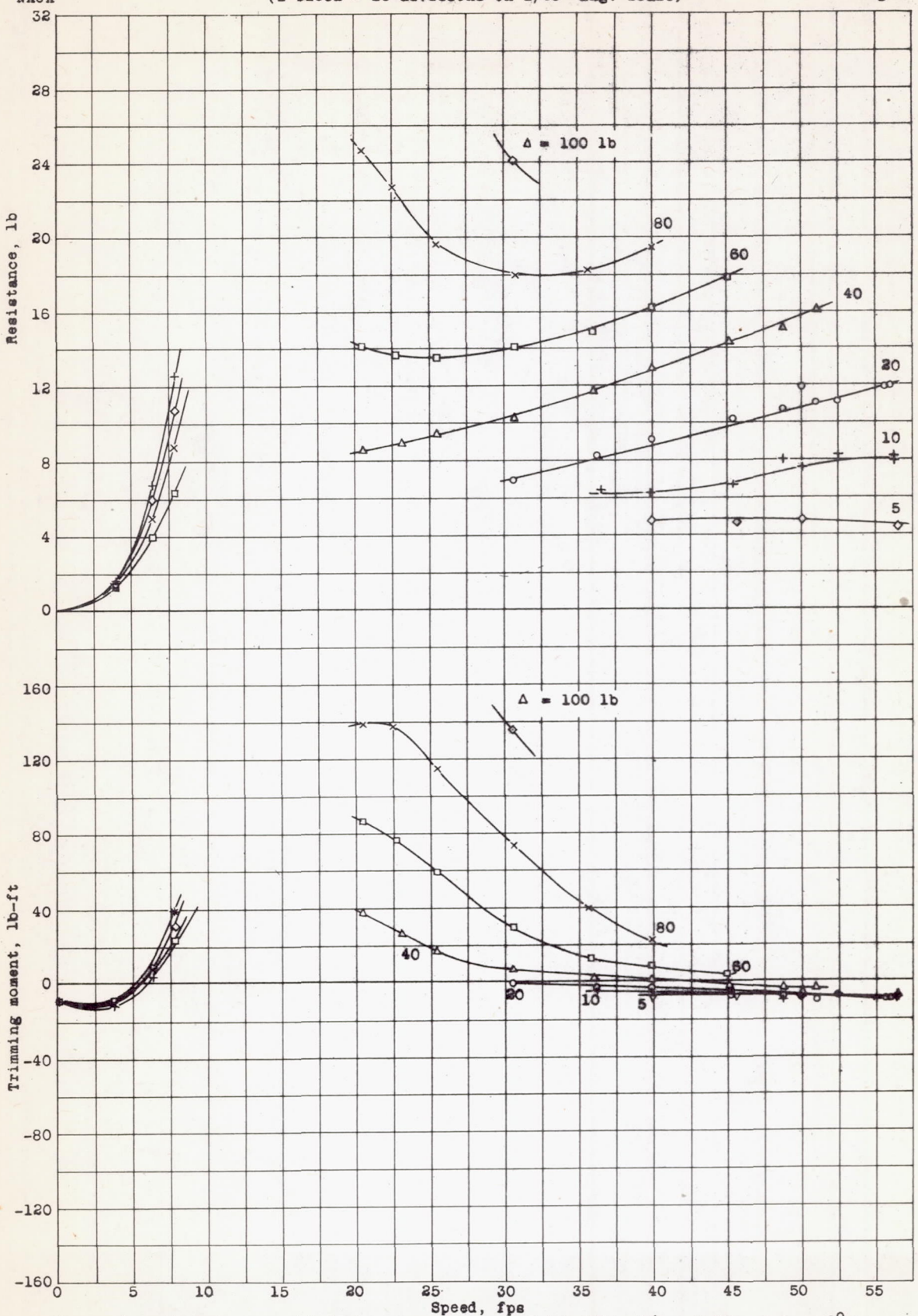

Figure 4. - Resistance and trimming moment. Model 144; L/b = 5.23; trim = 2°

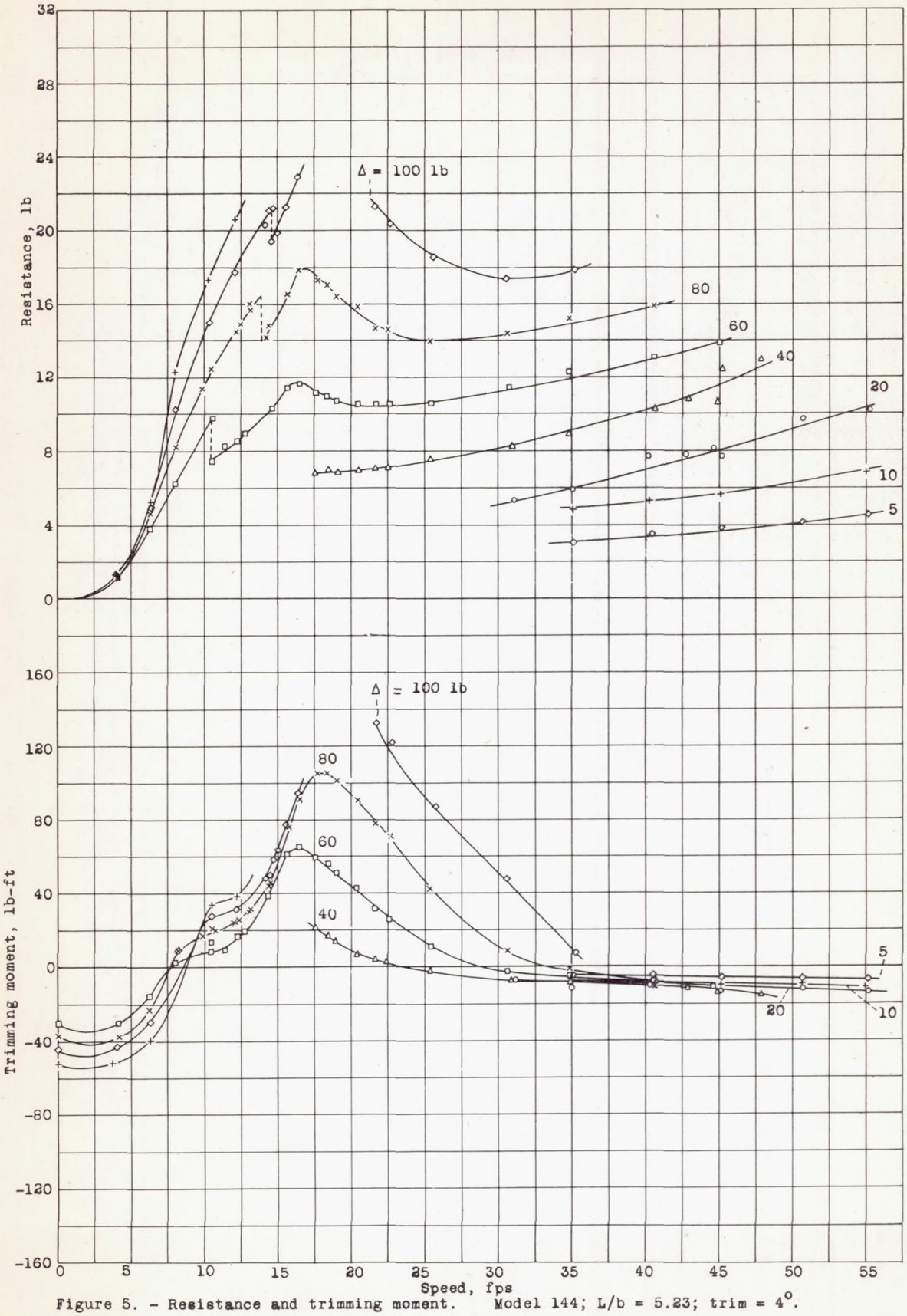

Figure 5. - Resistance and trimming moment. Model 144; L/b = 5.23; trim = 4°.

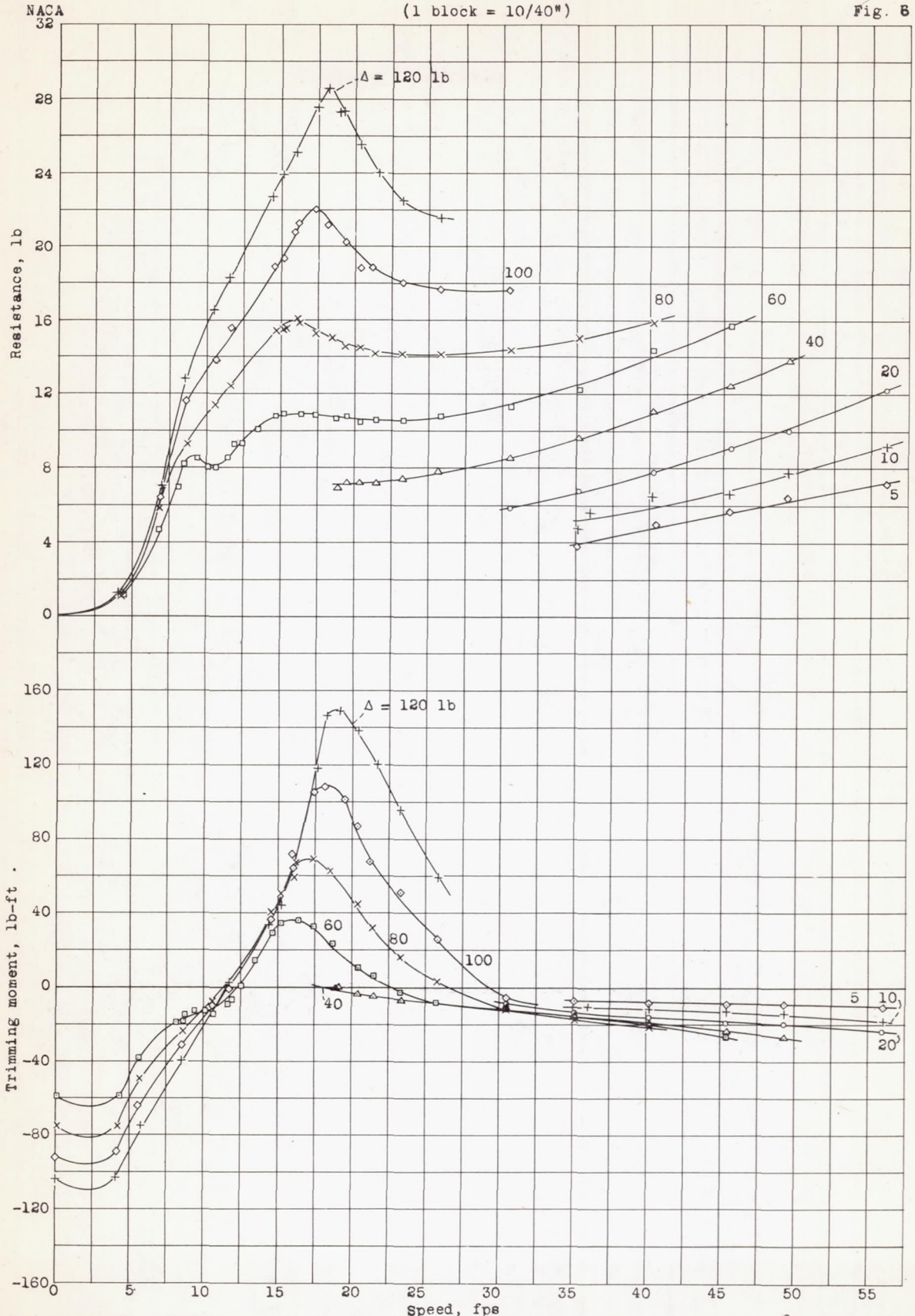

Figure 6. - Resistance and trimming moment. Model 144; L/b = 5.23; trim = 6°.

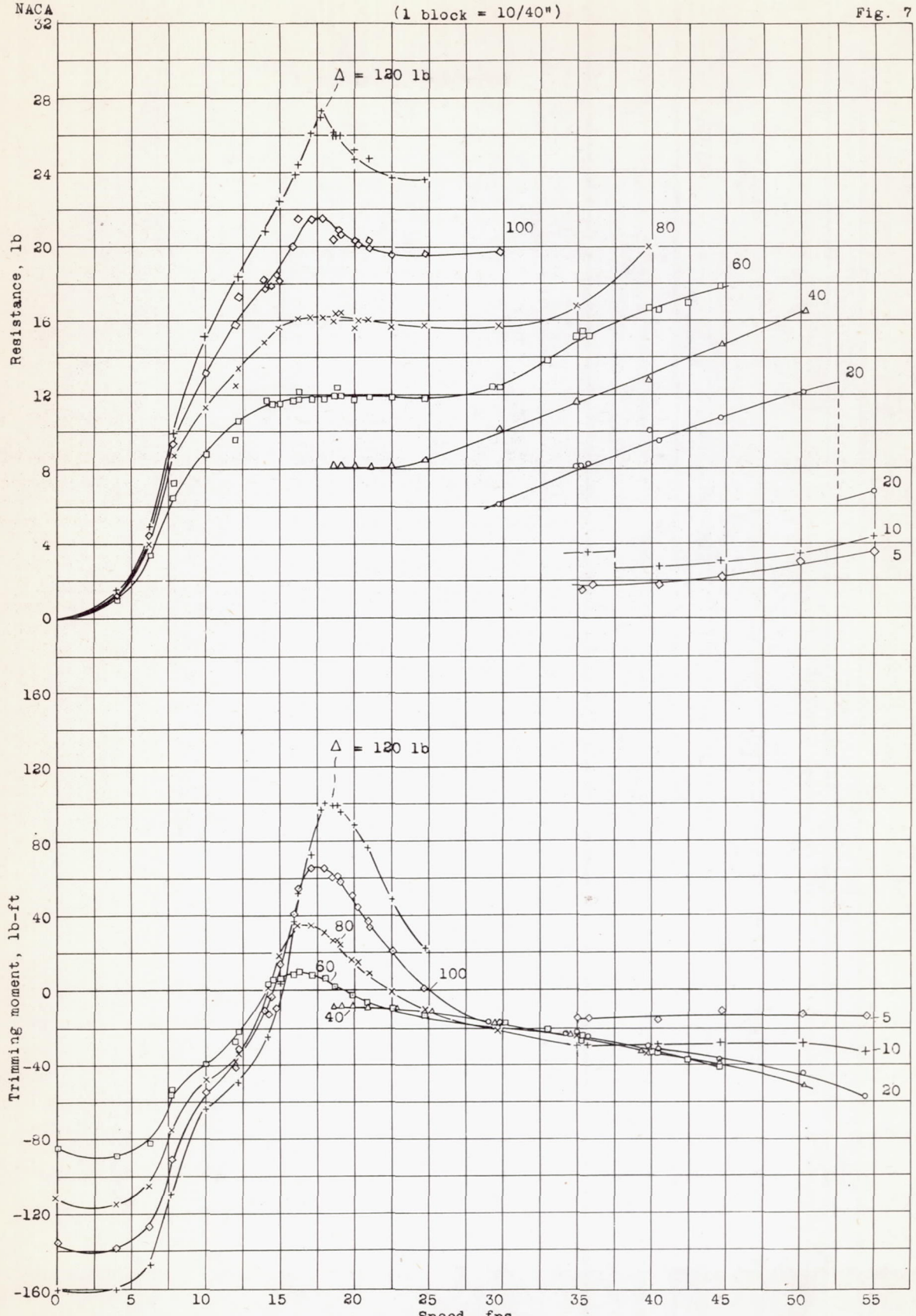

Figure 7.- Resistance and trimming moment. Model 144; L/b = 5.23; trim = 8°.

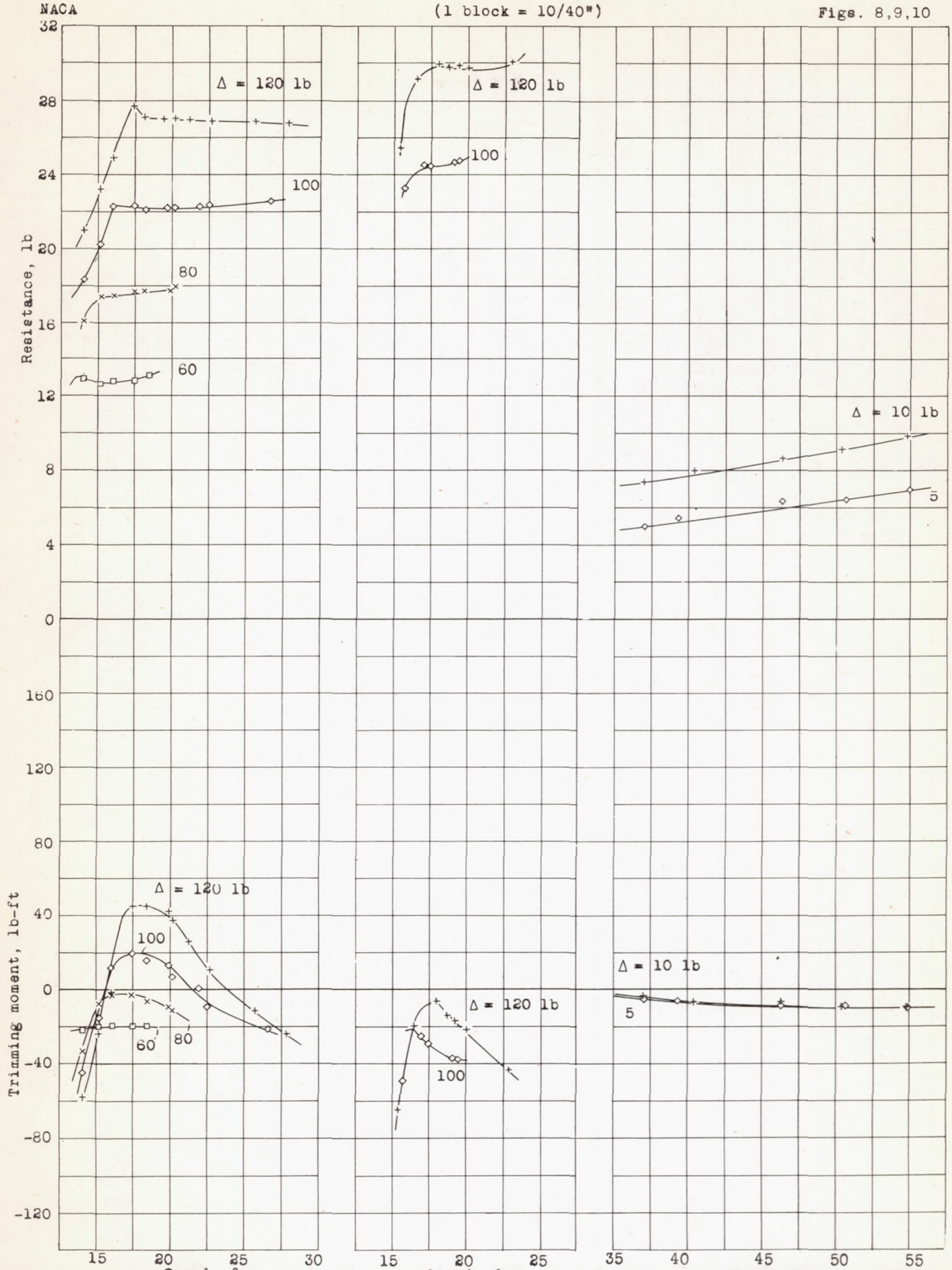

Figure 8.- Resistance and trimming moment.
Model 144; L/b = 5.23; trim = 10°

Fig.9.- Resistance and trimming moment.
Model 144; L/b = 5.23; trim = 12°.

Figure 10. - Resistance and trimming moment.
Model 145; L/b = 6.54; trim = 1°.

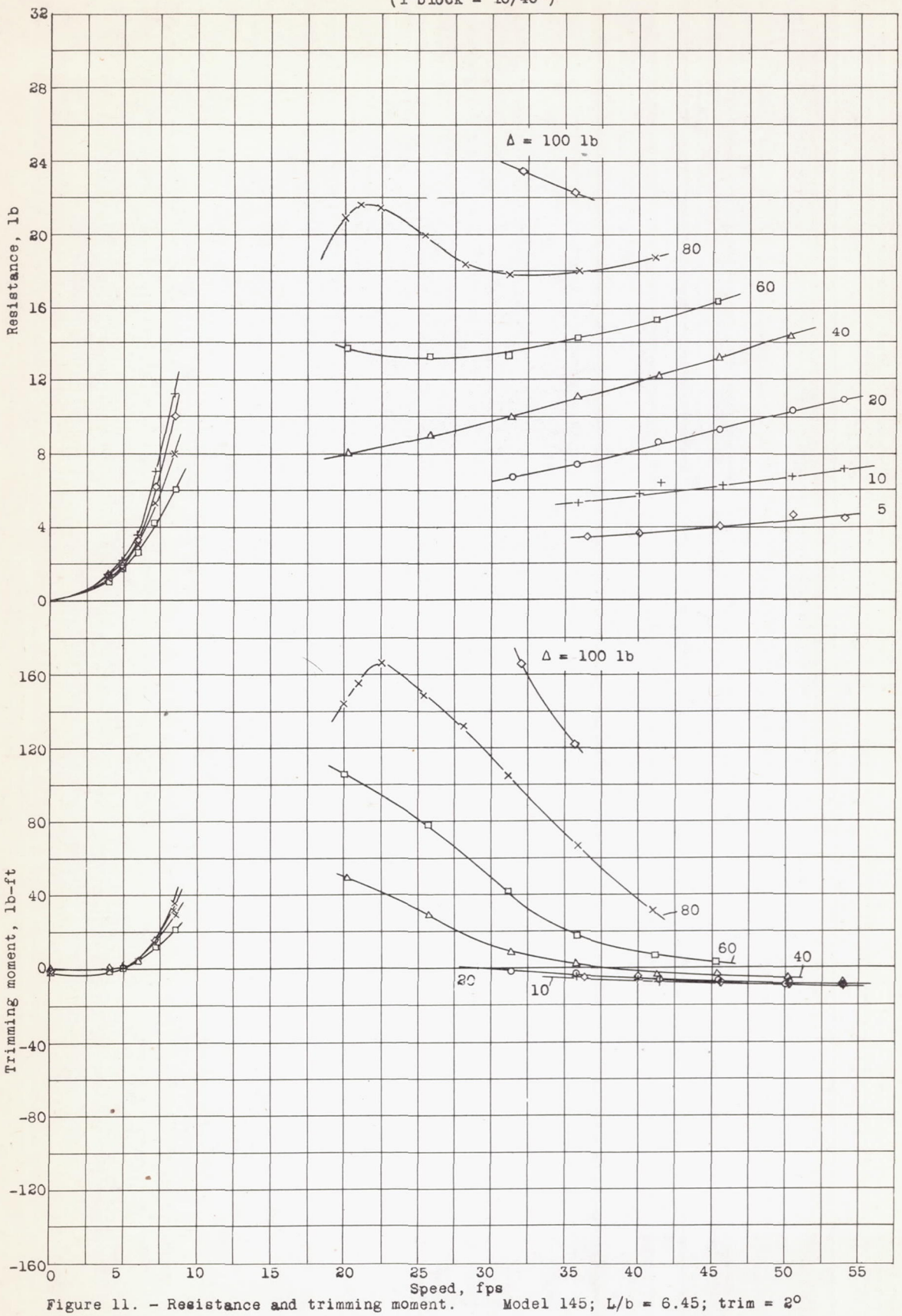

Figure 11. - Resistance and trimming moment. Model 145; L/b = 6.45; trim = 2°

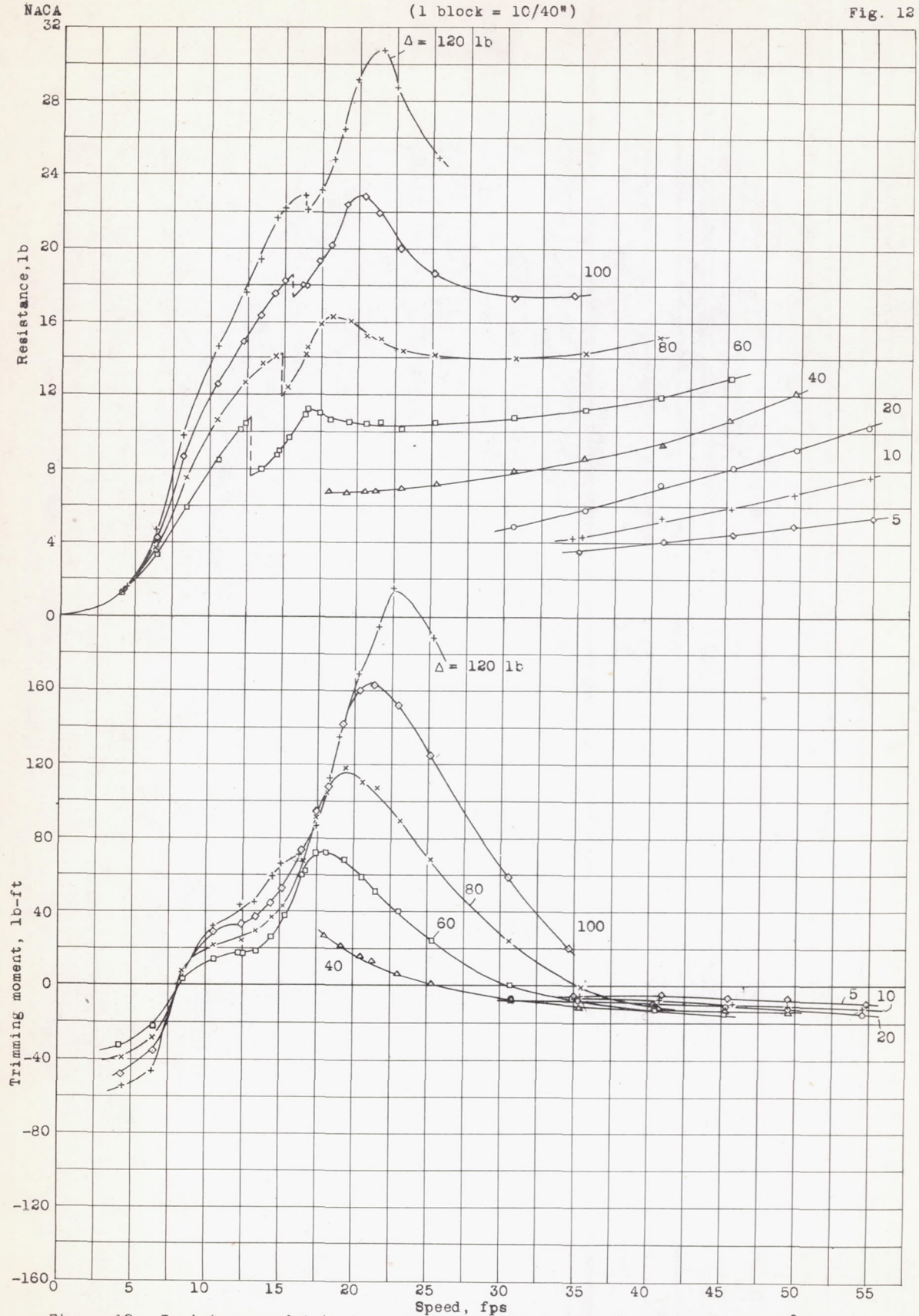

Figure 12.- Resistance and trimming moment. Model 145; L/b = 6.54; trim = 4°.

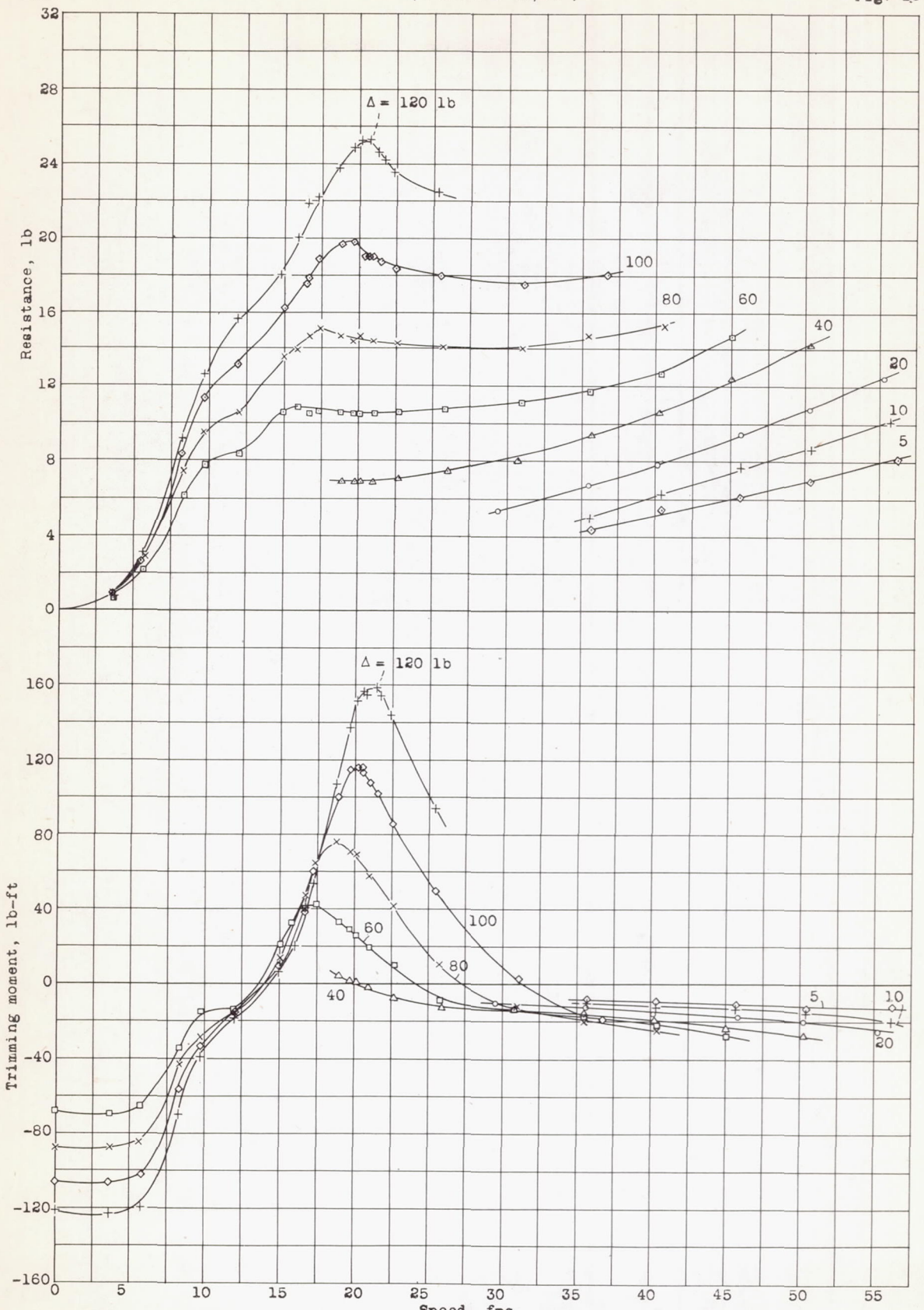

Figure 13.- Resistance and trimming moment. Model 145; L/b = 6.54; trim = 6°.

NACA (1 block = 10/40") Fig. 14

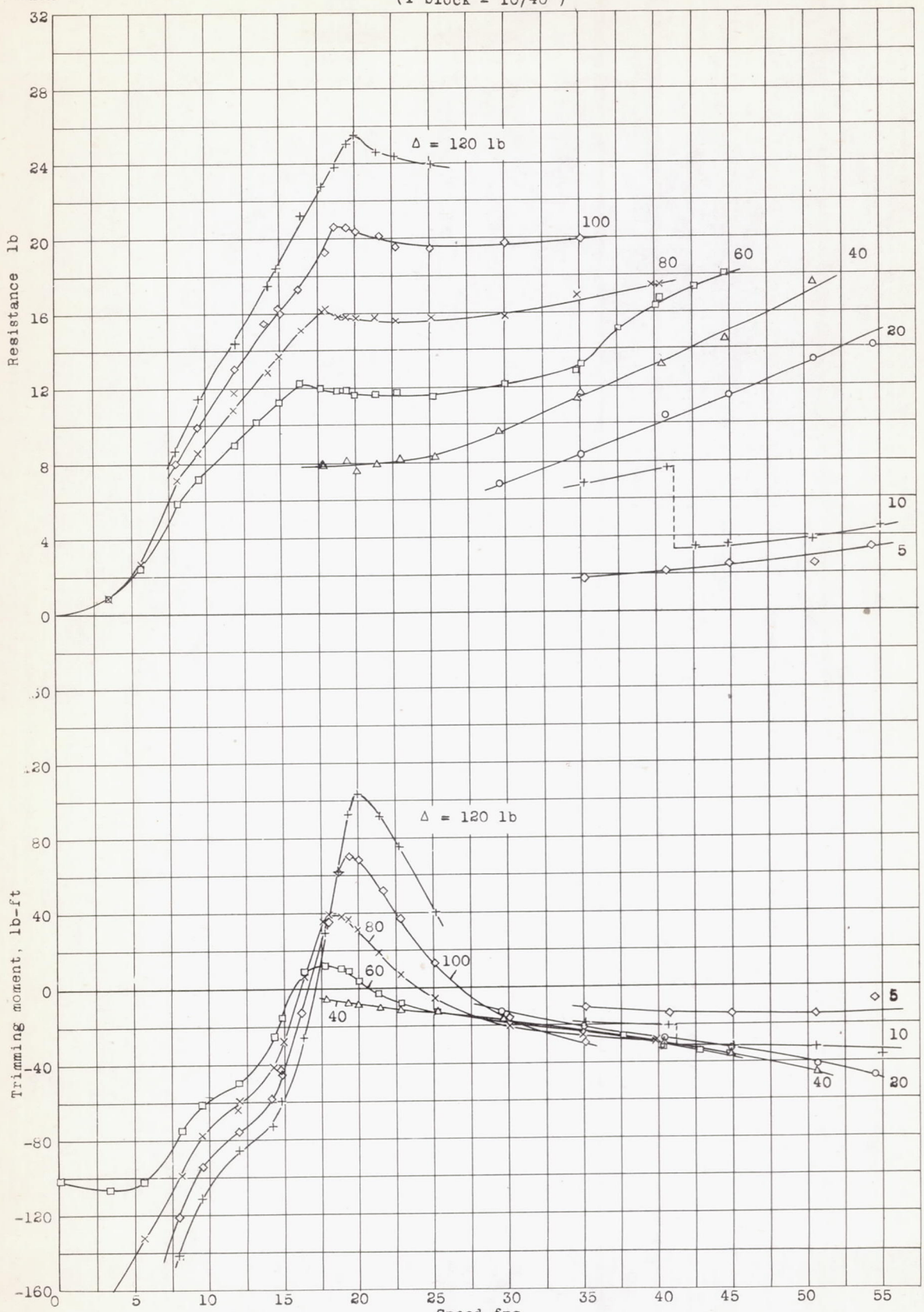

Figure 14.- Resistance and trimming moment. Model 145; L/b = 6.54; trim = 8°

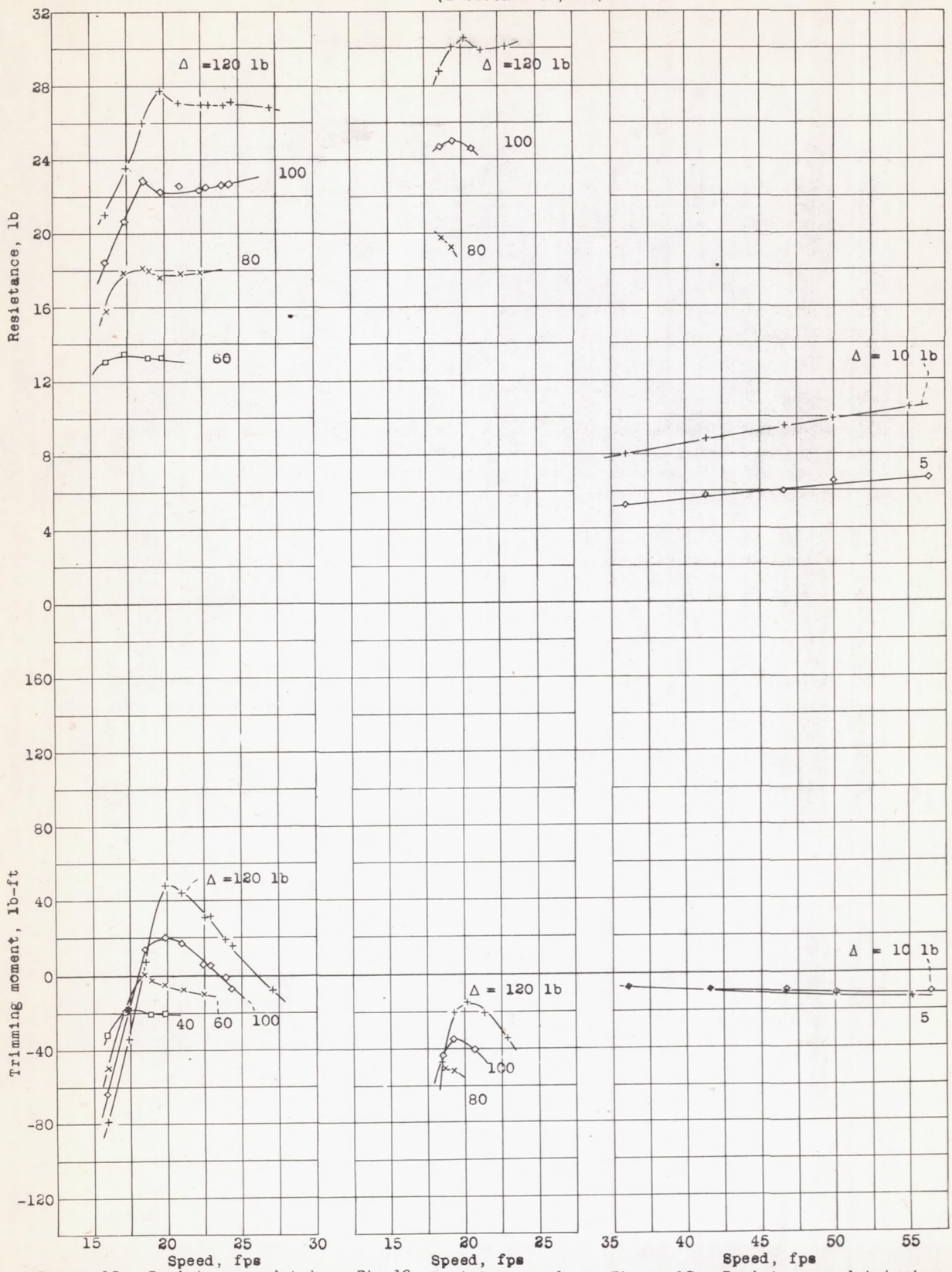

Figure 15.- Resistance and trimming moment.
Model 145; L/b = 6.54; trim = 10°.

Fig.16.-Resistance and trimming moment.
Model 145; L/b = 6.54; trim = 12°.

Figure 17.- Resistance and trimming moment.
Model 146; L/b = 7.84; trim = 1°.

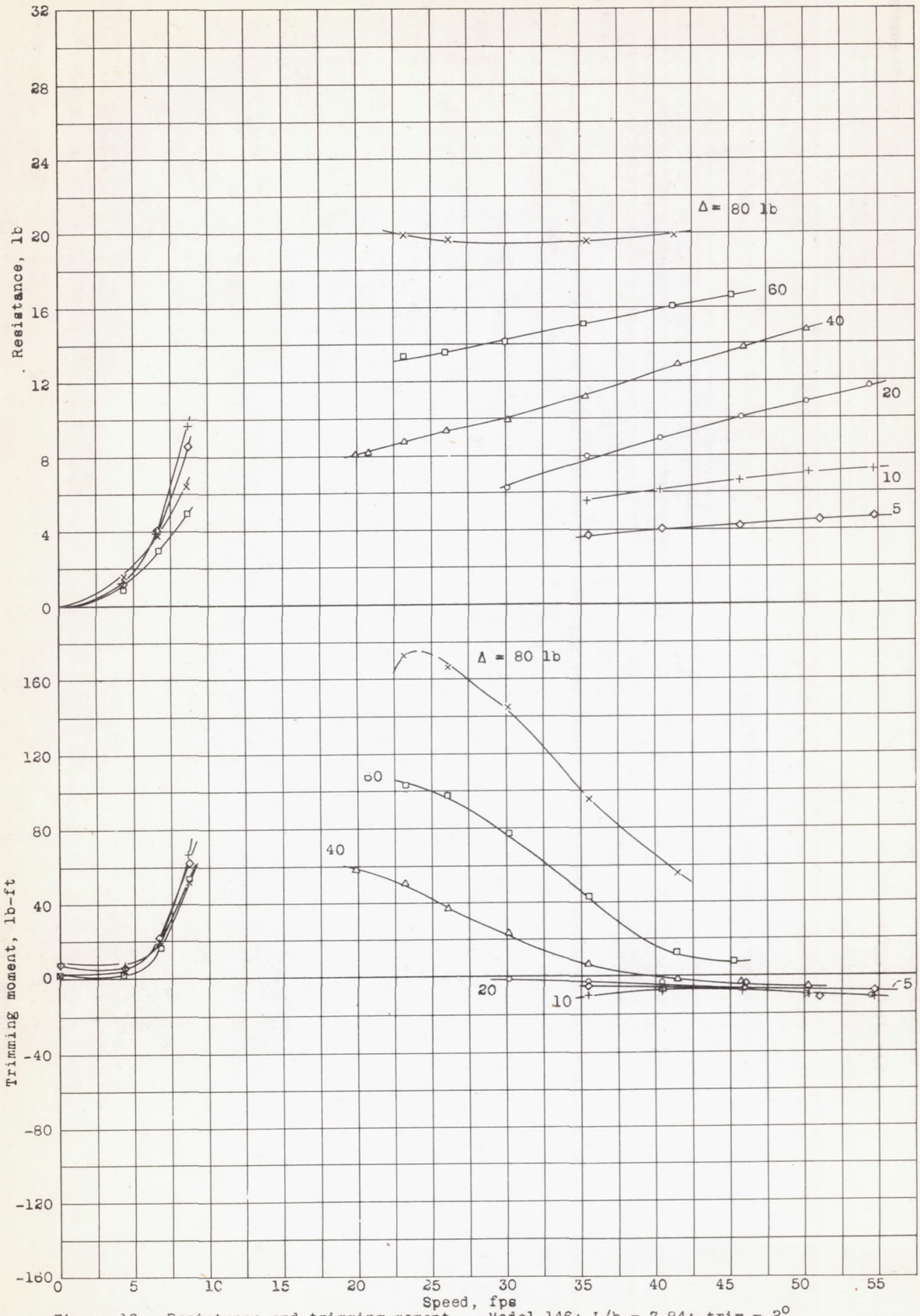

Figure 18.- Resistance and trimming moment. Model 146; L/b = 7.84; trim = 2°.

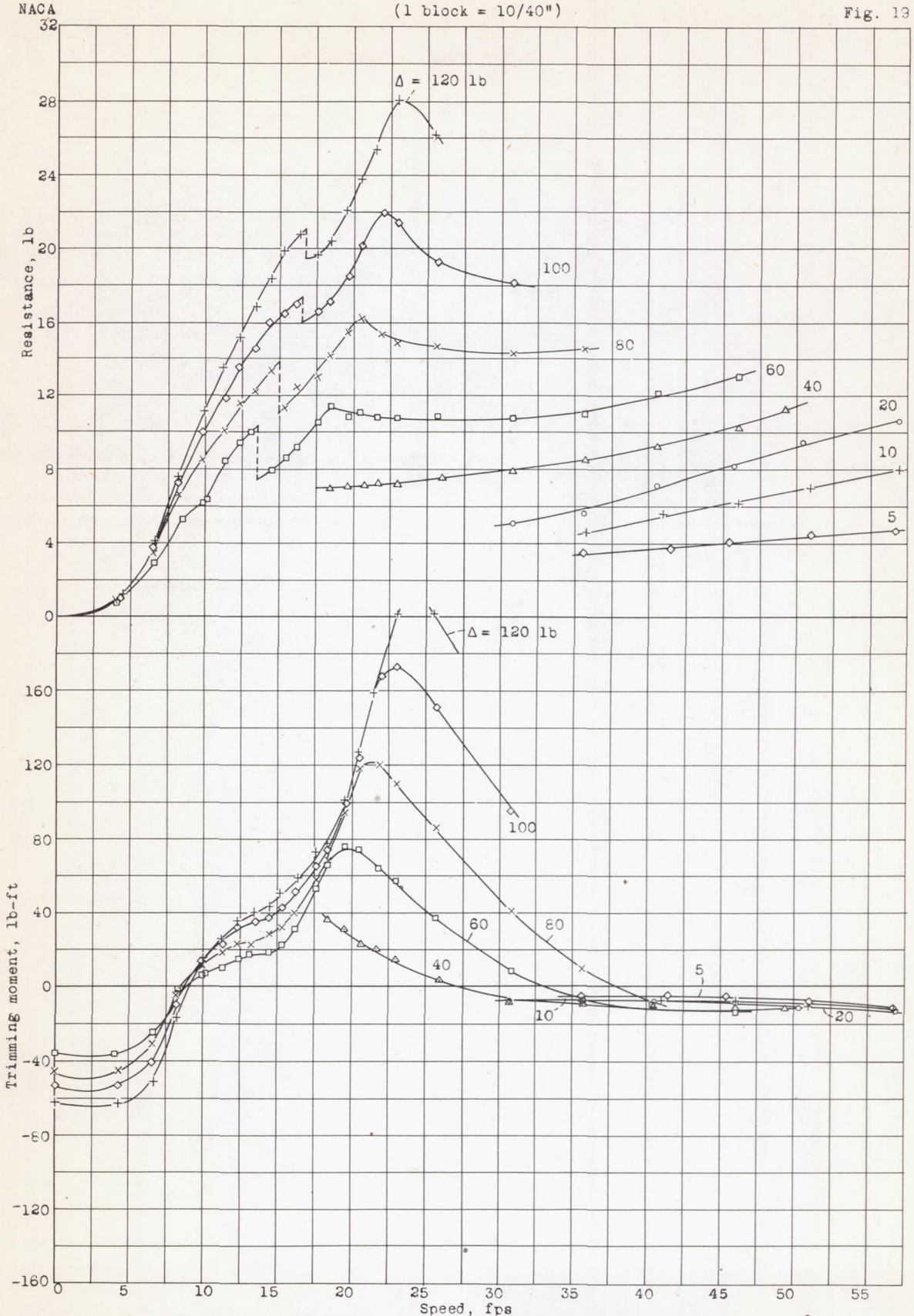

Figure 19.- Resistance and trimming moment. Model 146; L/b = 7.84; trim = 4°.

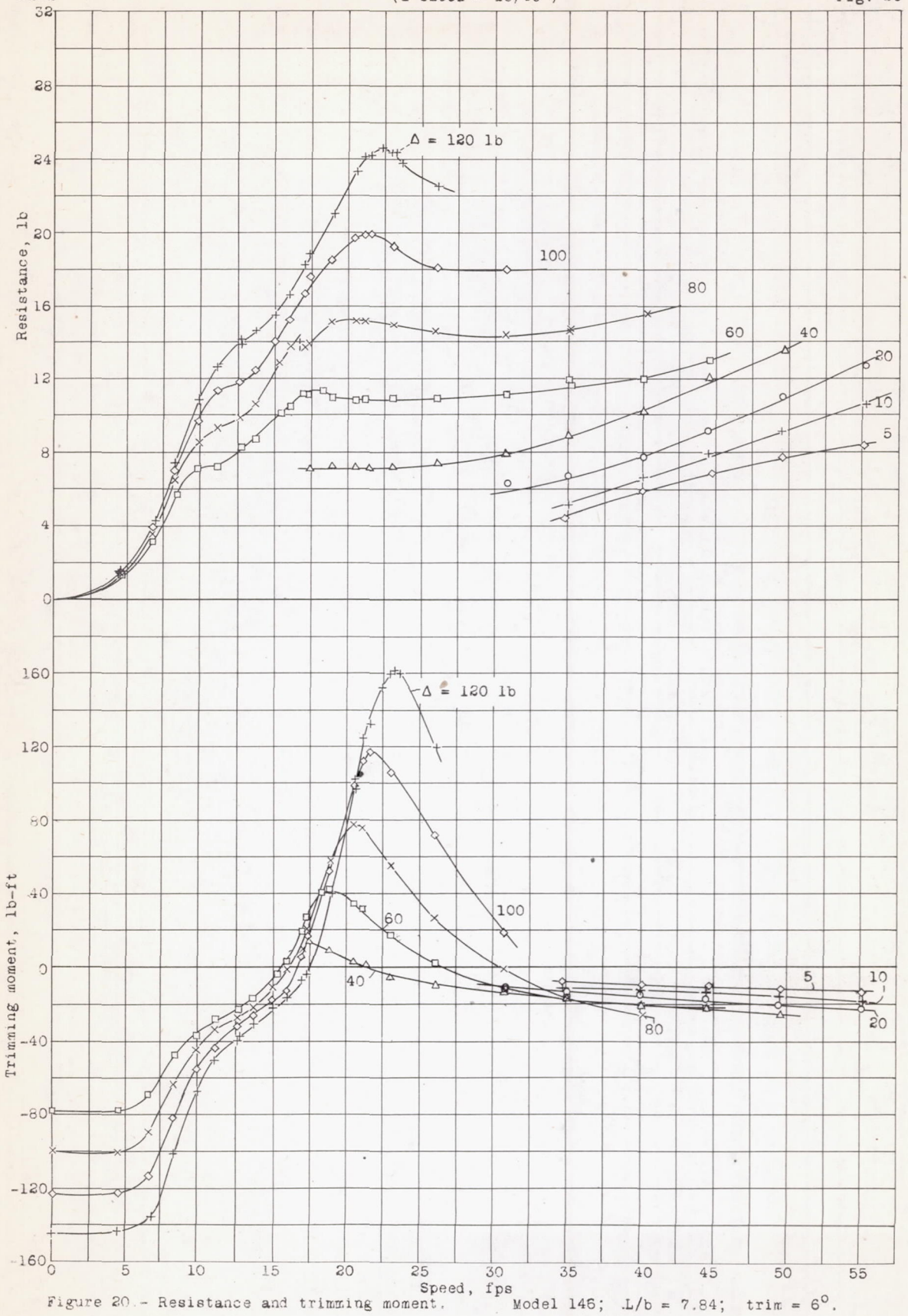

Figure 20.- Resistance and trimming moment. Model 146; L/b = 7.84; trim = 6°.

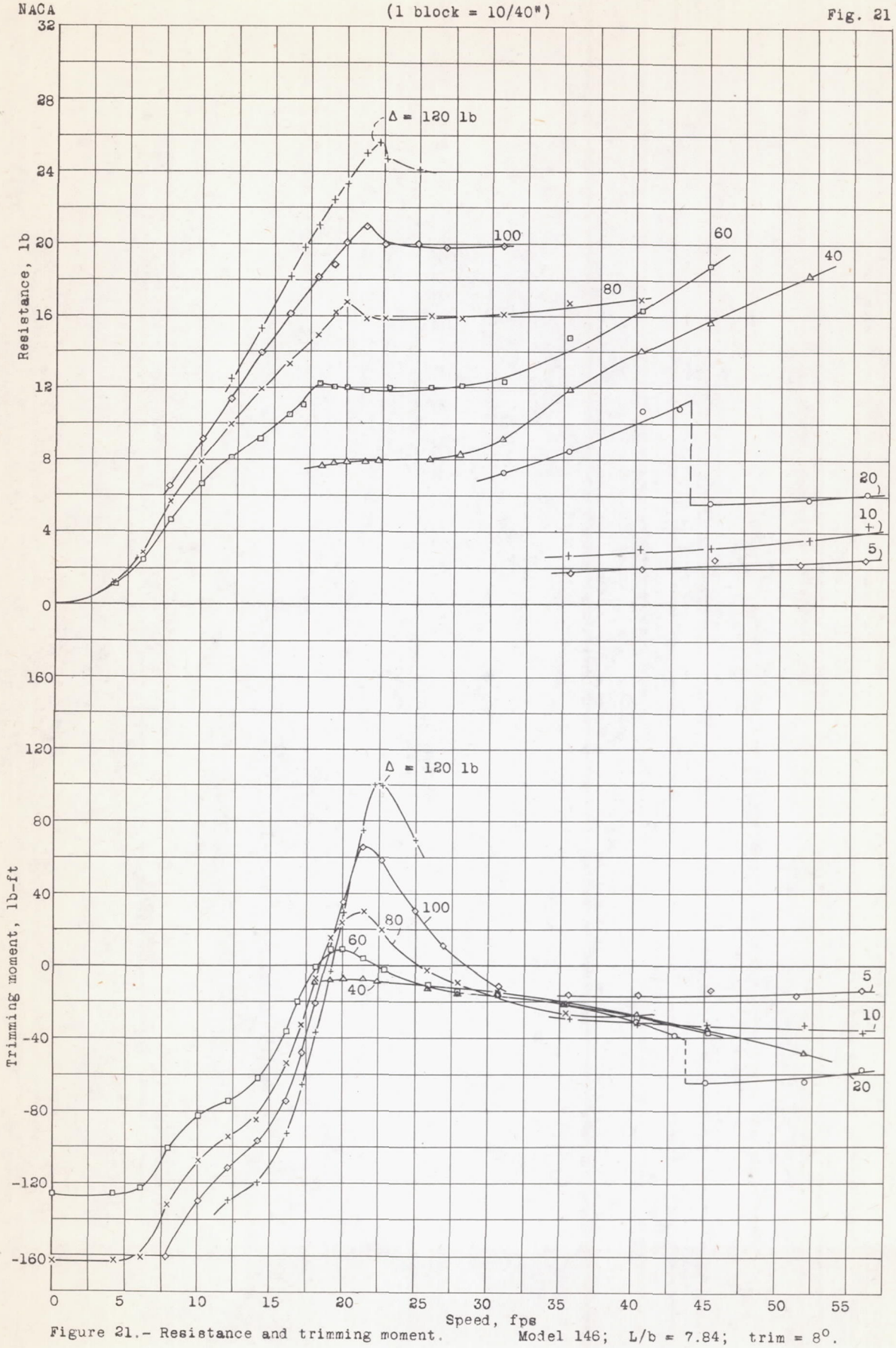

Figure 21.- Resistance and trimming moment. Model 146; L/b = 7.84; trim = 8°.

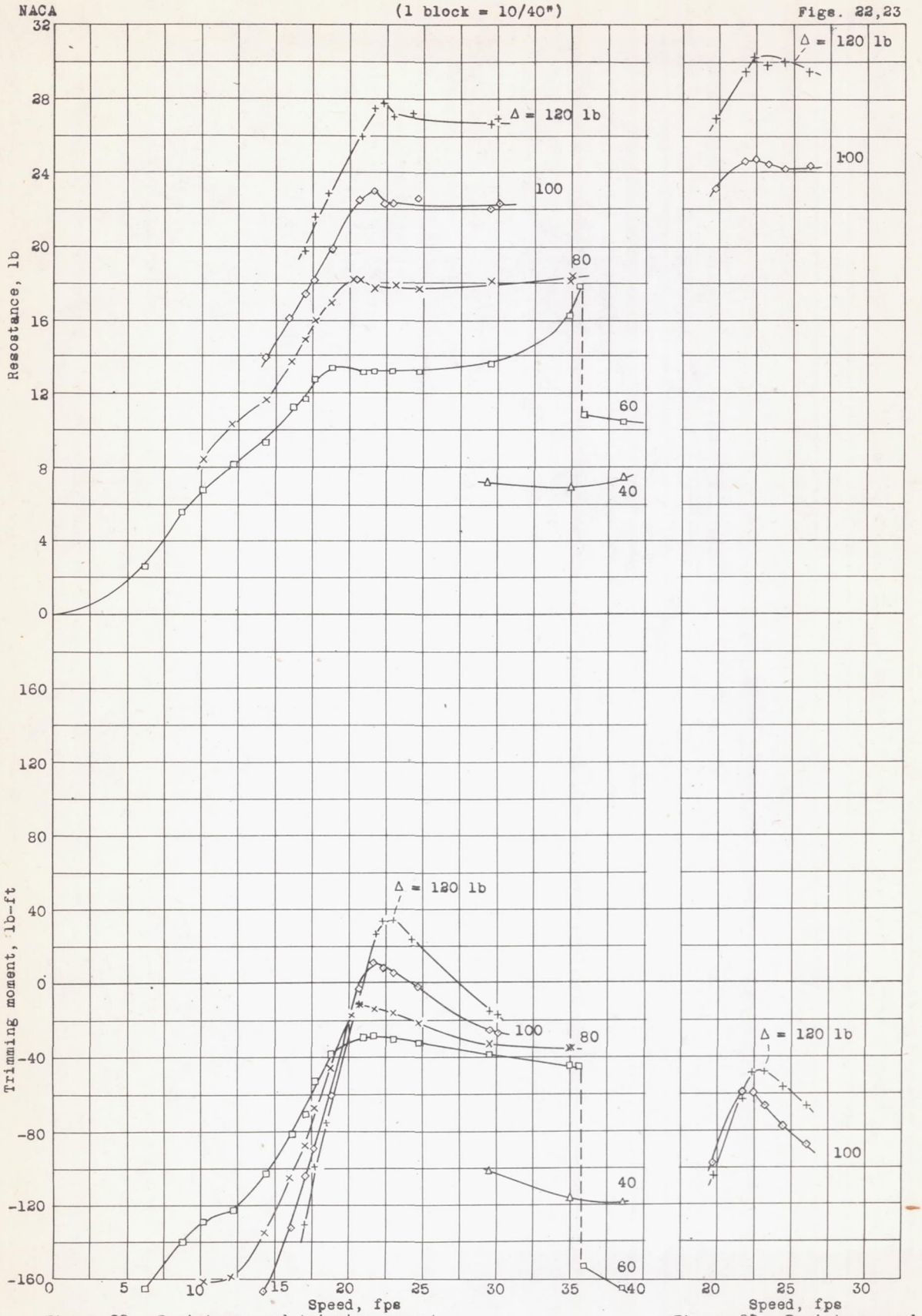

Figure 22.- Resistance and trimming moment.
Model 146; L/b = 7.84; trim = 10°.

Figure 23.- Resistance and trimming moment.
Model 146; L/b = 7.84; trim = 12°.

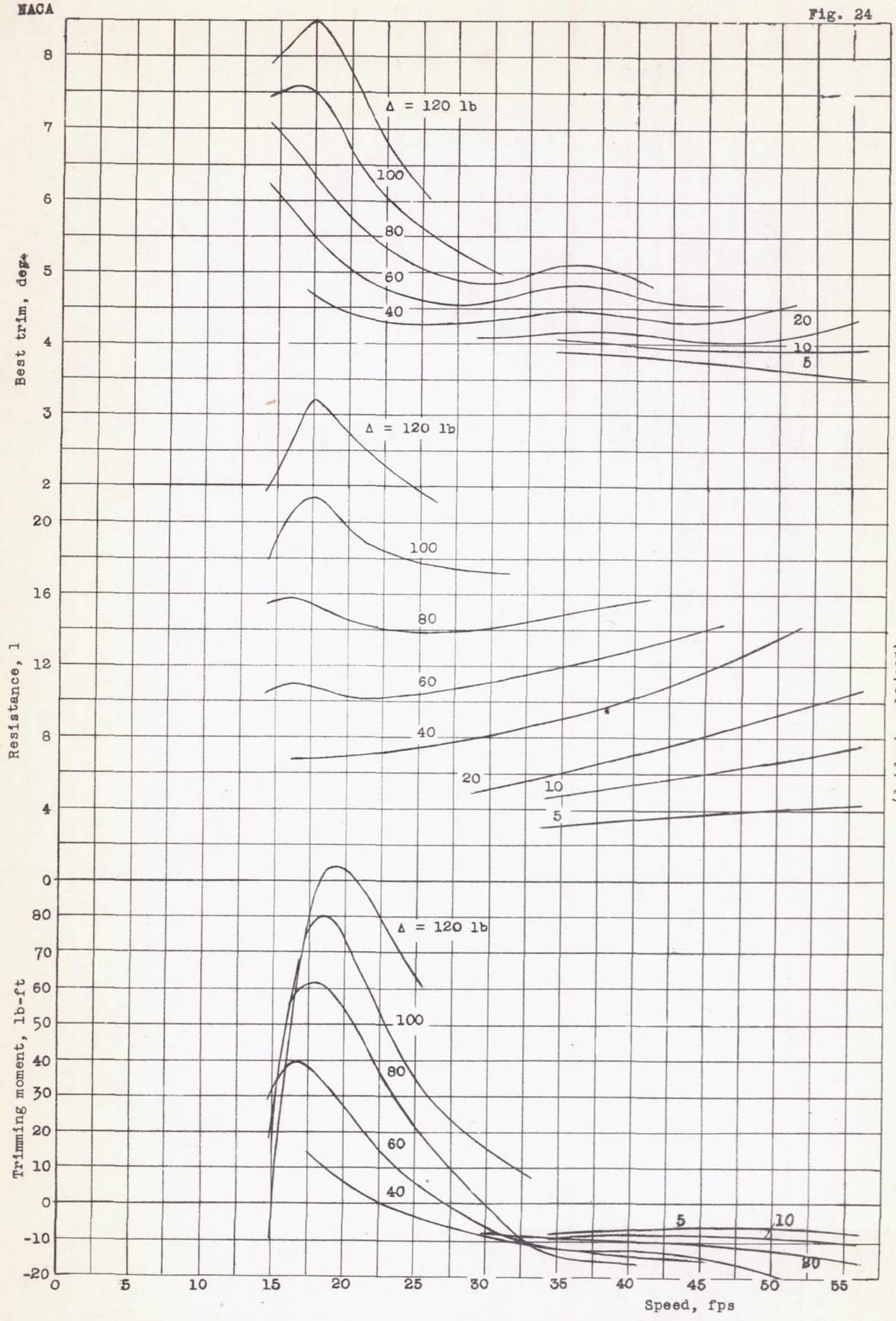

Figure 24.- Variation of best trim, resistance at best trim, and trimming moment at best trim with speed. Model 144; L/b = 5.23.

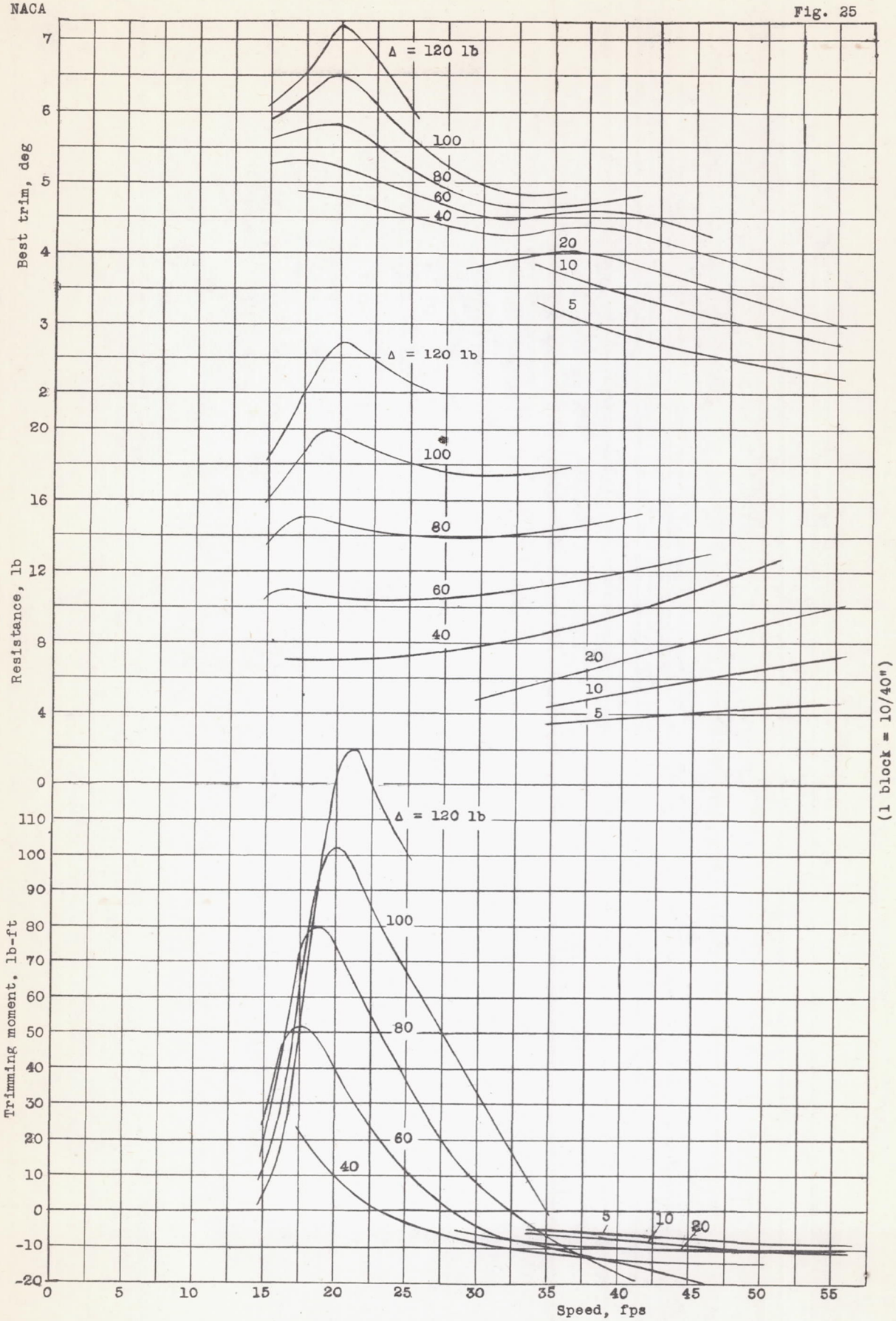

Figure 25.- Variation of best trim, resistance at best trim, and trimming moment at best trim with speed. Model 145; L/b = 6.54.

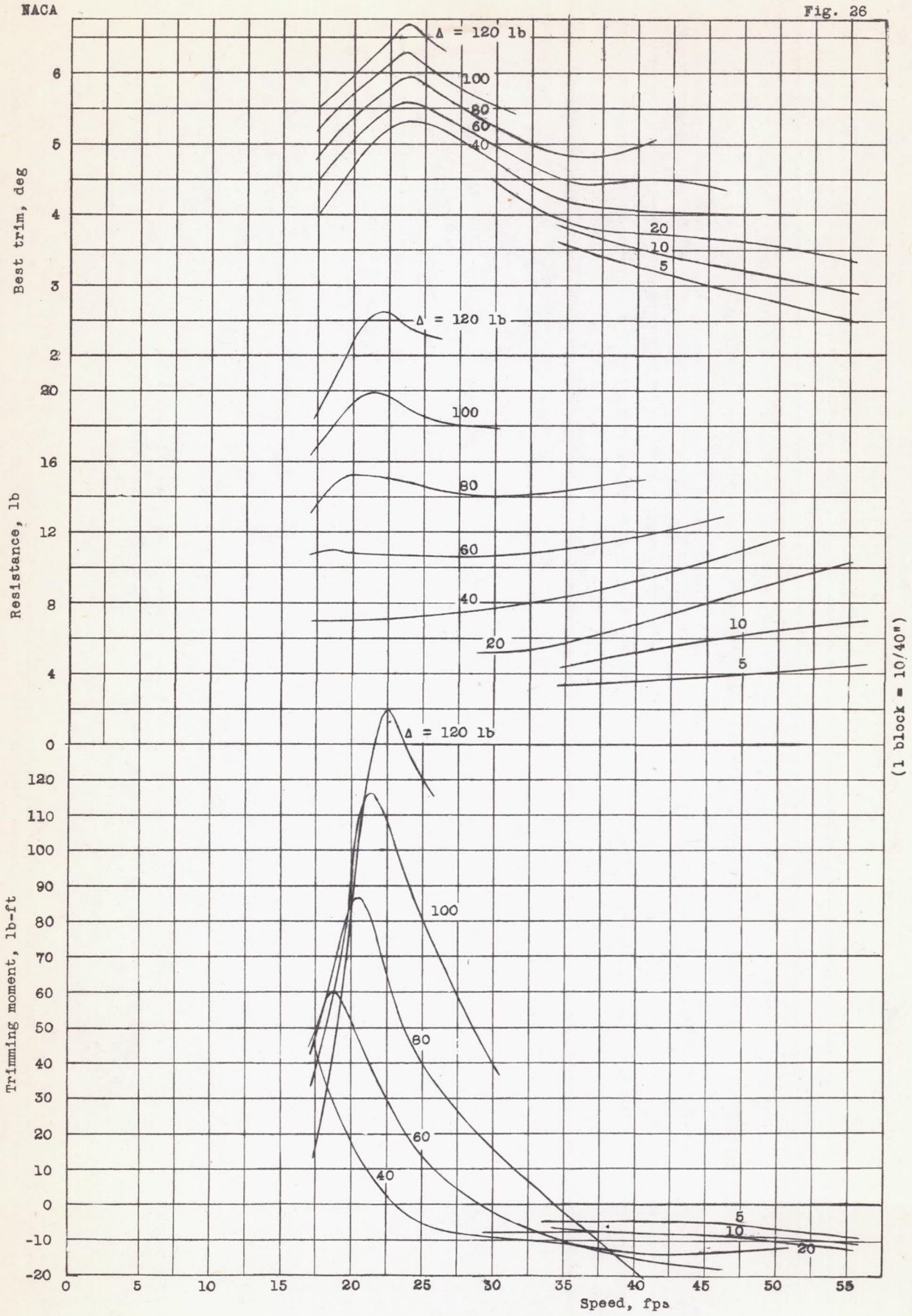

Figure 26.- Variation of best trim, resistance at best trim, and trimming moment at best trim with speed. Model 146; L/b = 7.84.

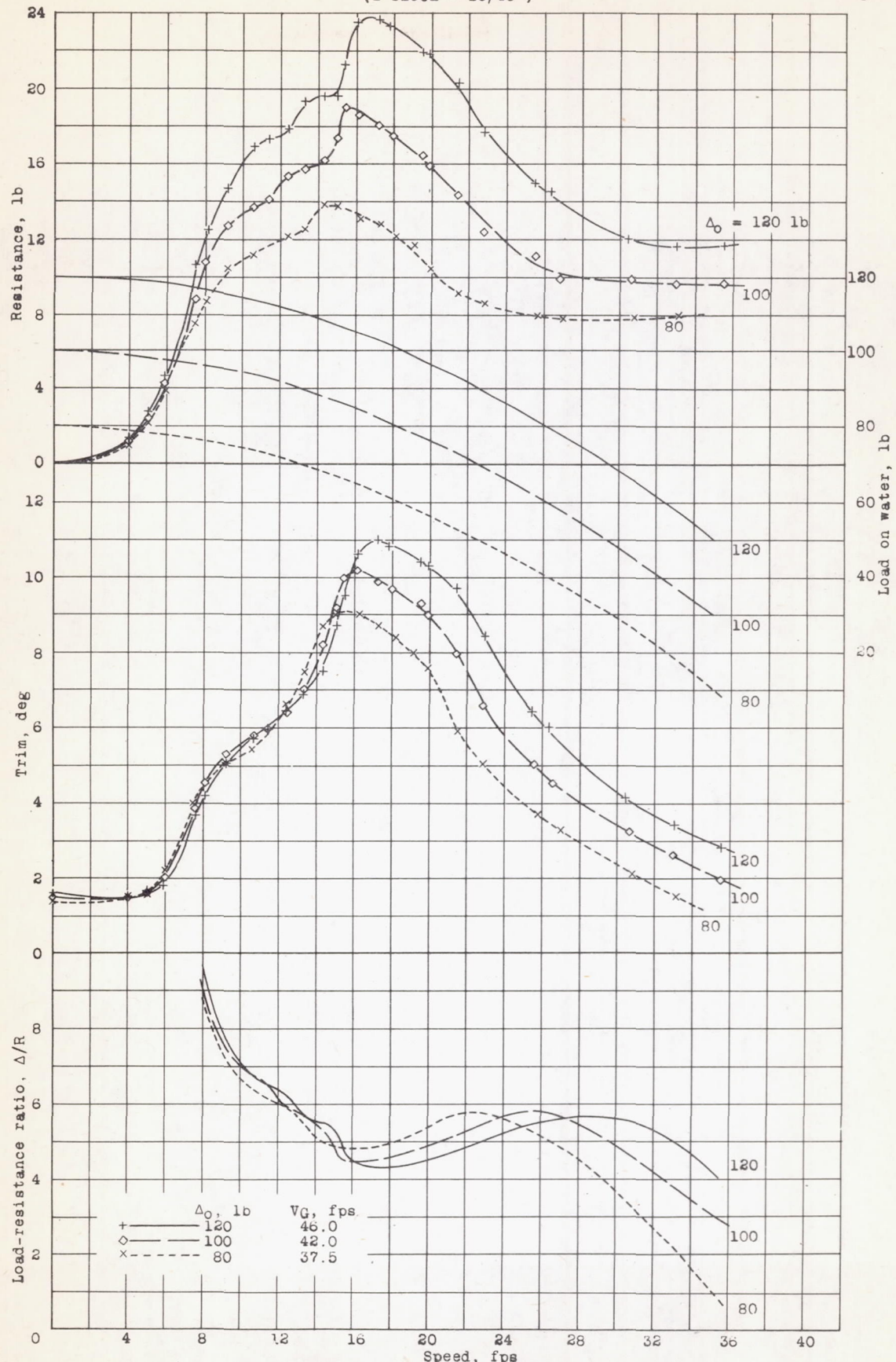

Figure 27.- Specific free-to-trim tests. Model 144; L/b = 5.23.

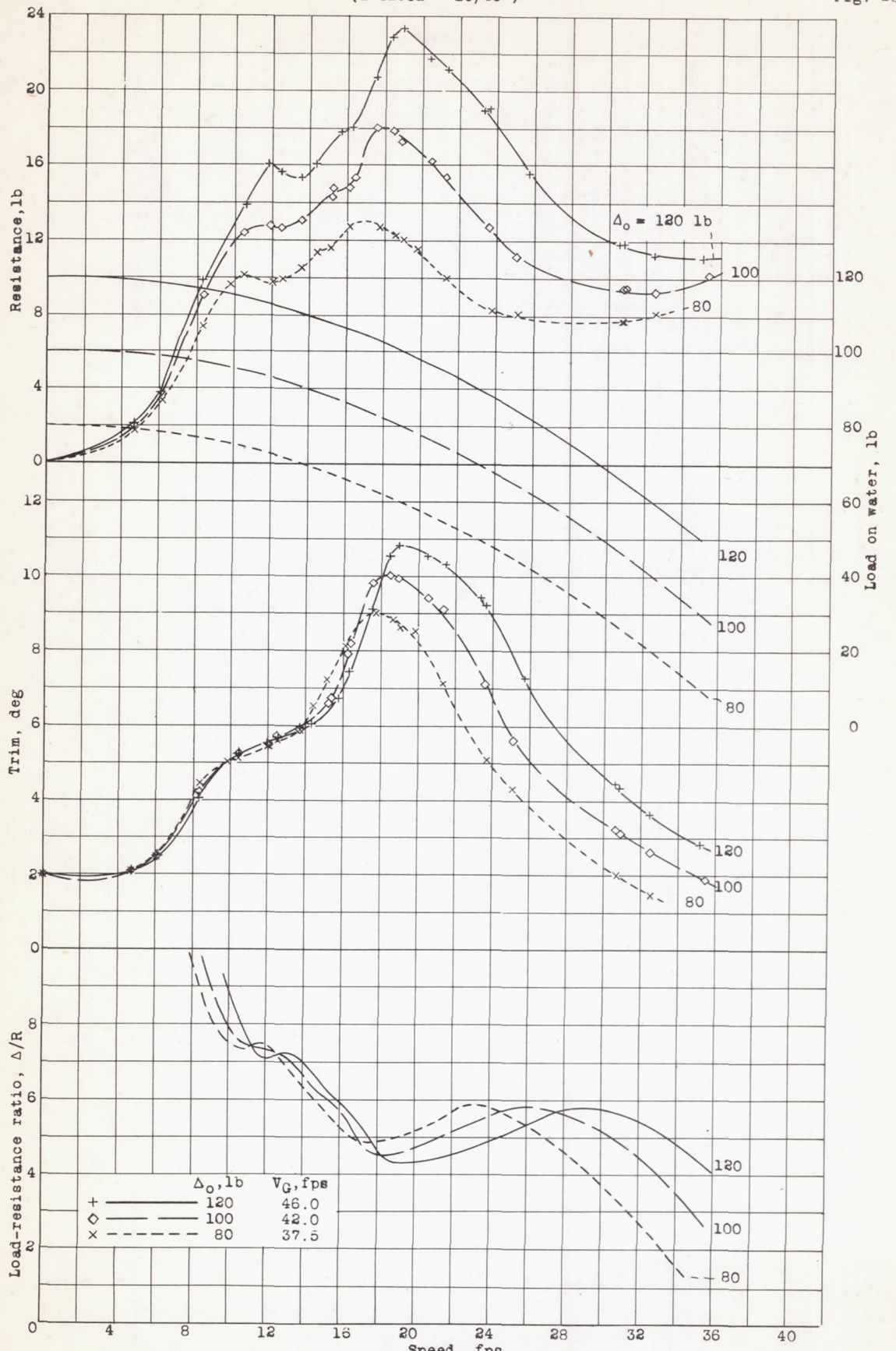

Figure 28.- Specific free-to-trim tests. Model 145; L/b = 6.54.

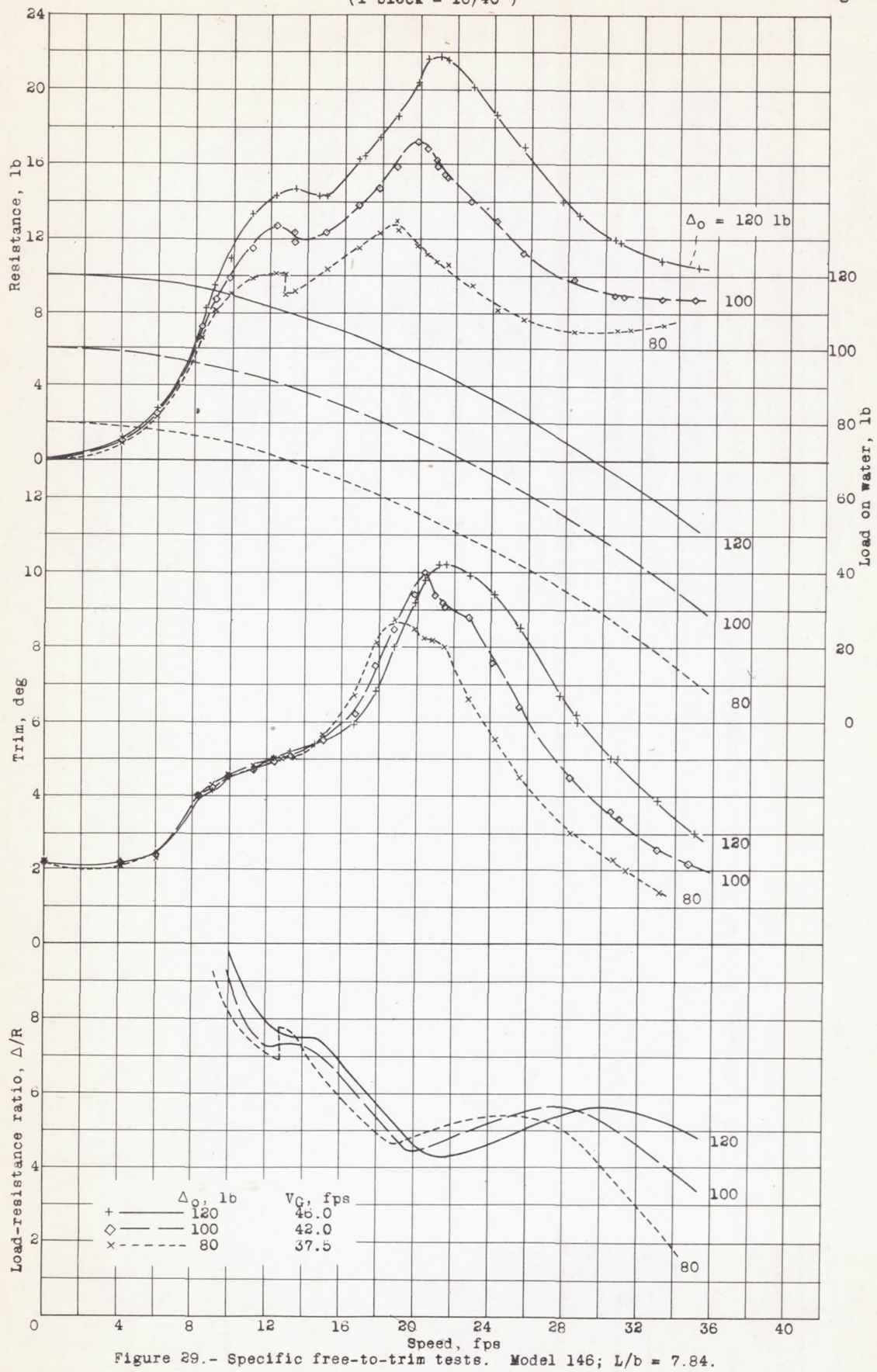

Figure 29.- Specific free-to-trim tests. Model 146; L/b = 7.84.

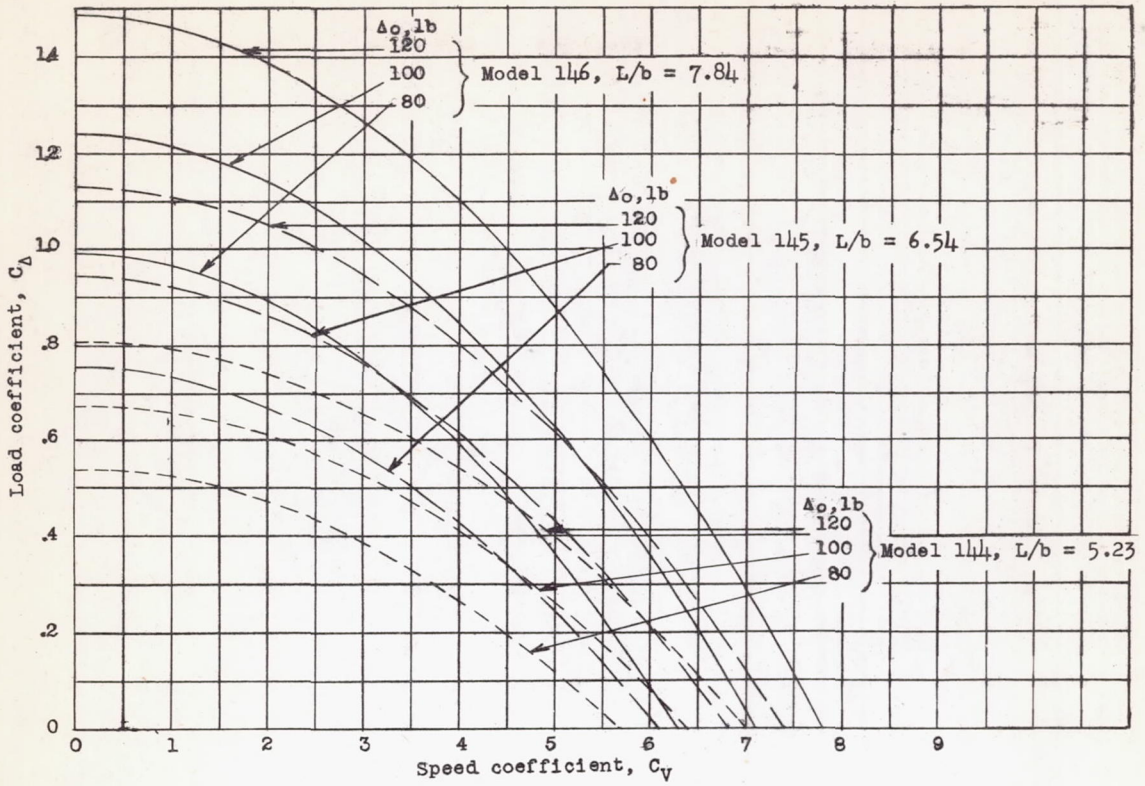

Figure 30.- Variation of load coefficient with speed coefficient for free-to-trim tests of models 144, 145, and 146.

(1 block = 10/40")

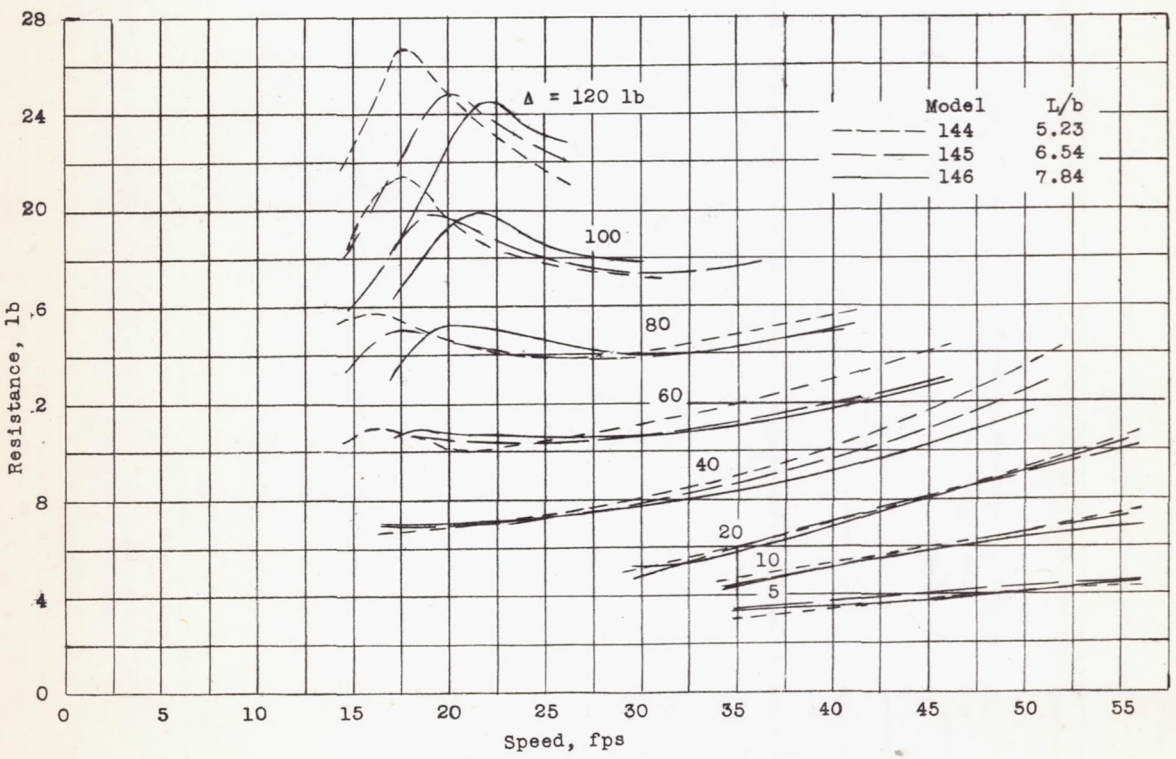

Figure 31.- Effect of length-beam ratio on resistance at best trim.

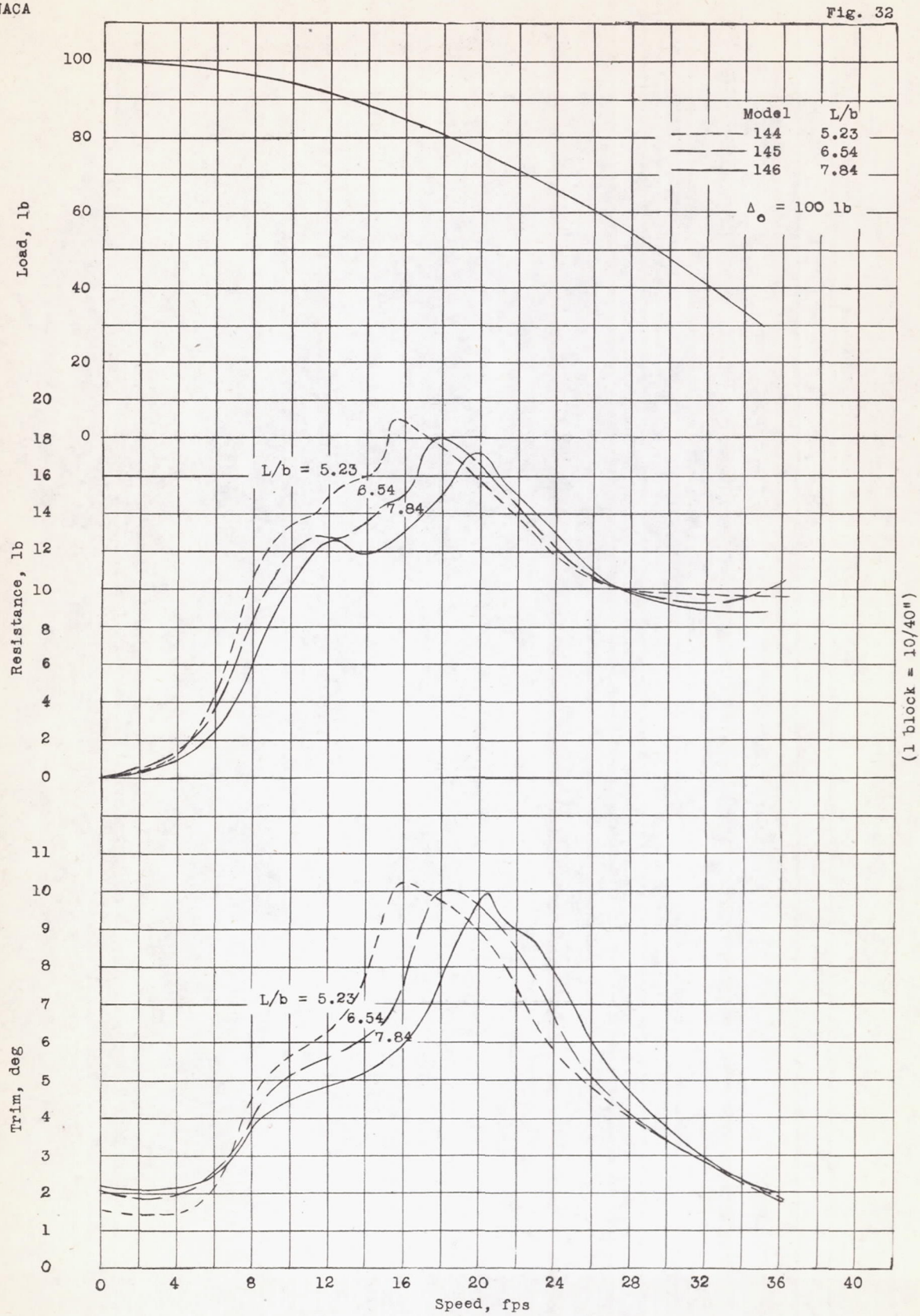

Figure 32.- Effect of length-beam ratio on trim and resistance in free-to-trim condition.

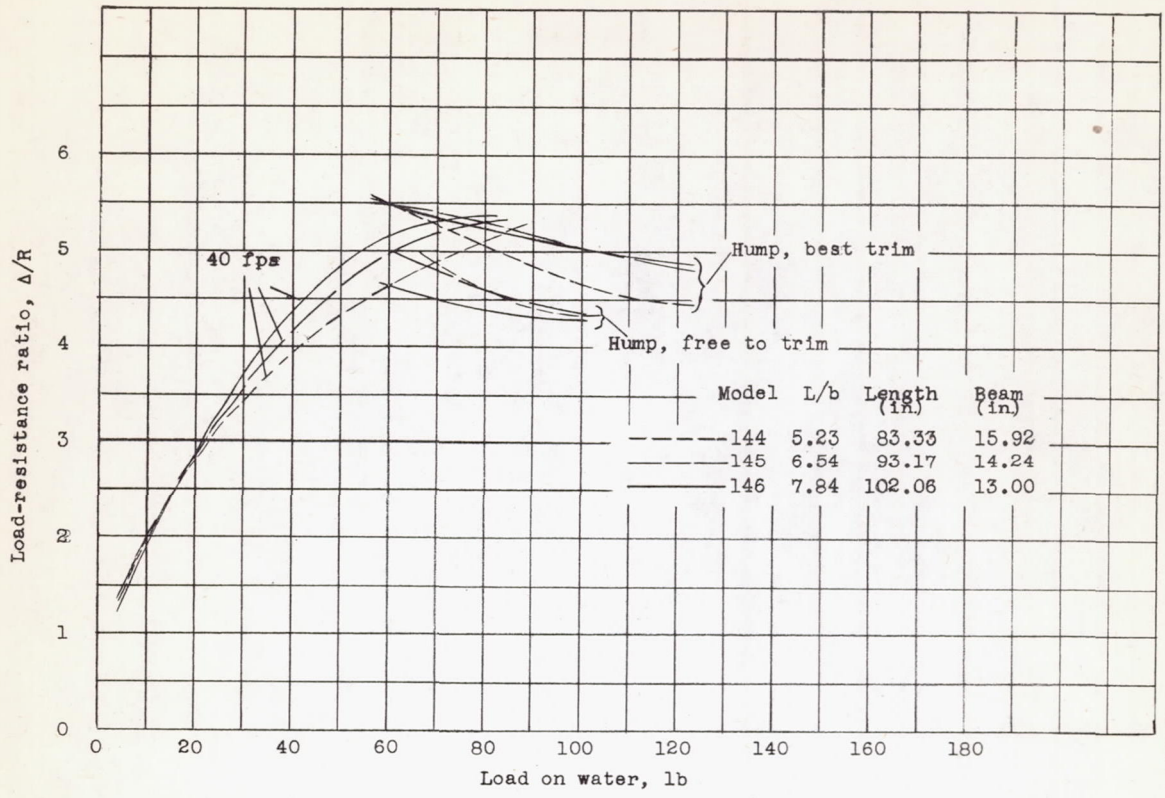

(a) Effect of varying length-beam ratio with constant length-beam product.

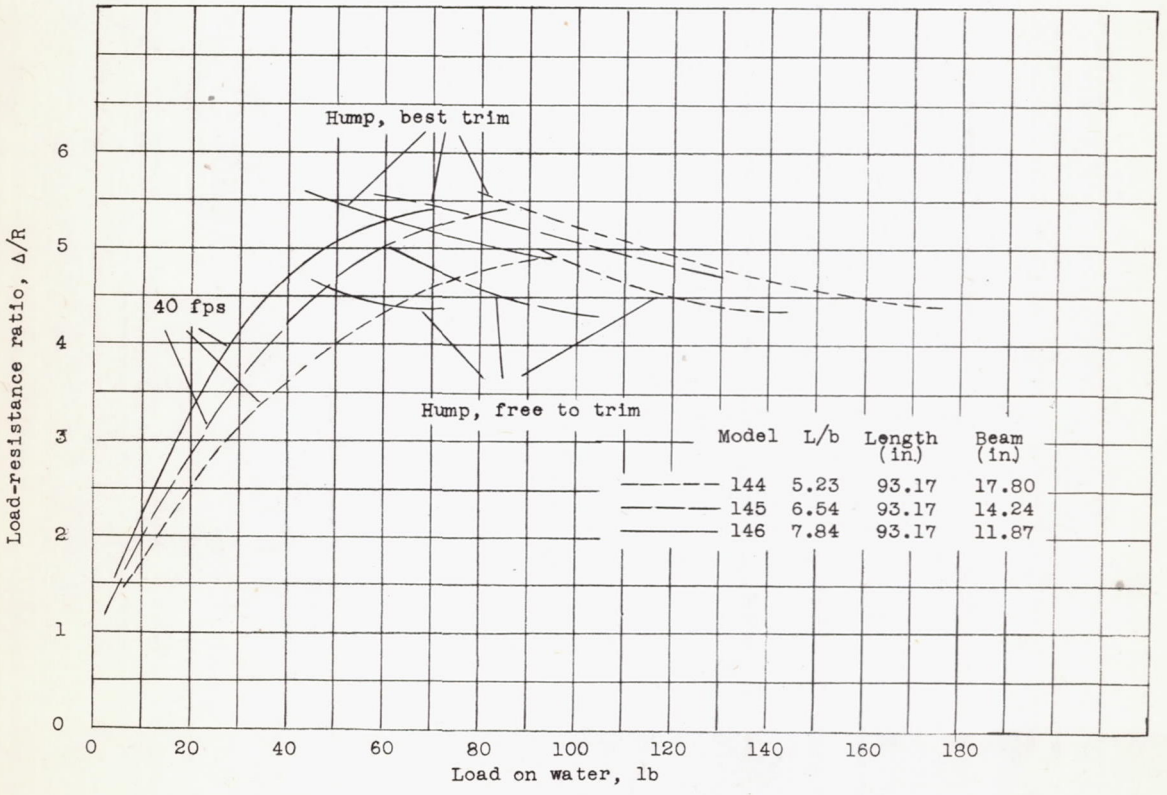

(b) Effect of change in beam.

Figure 33.- Variation of load-resistance ratio with load for different length-beam ratios.

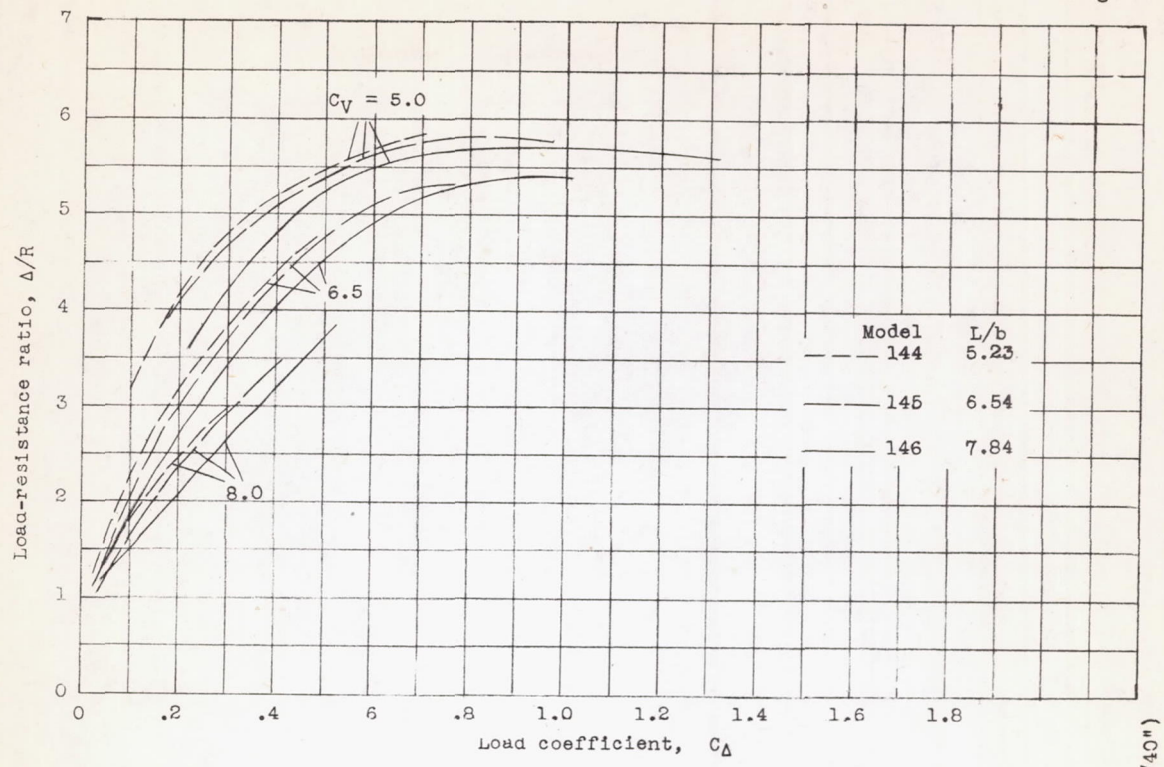

(a) Variation at speeds above hump speed, best trim.

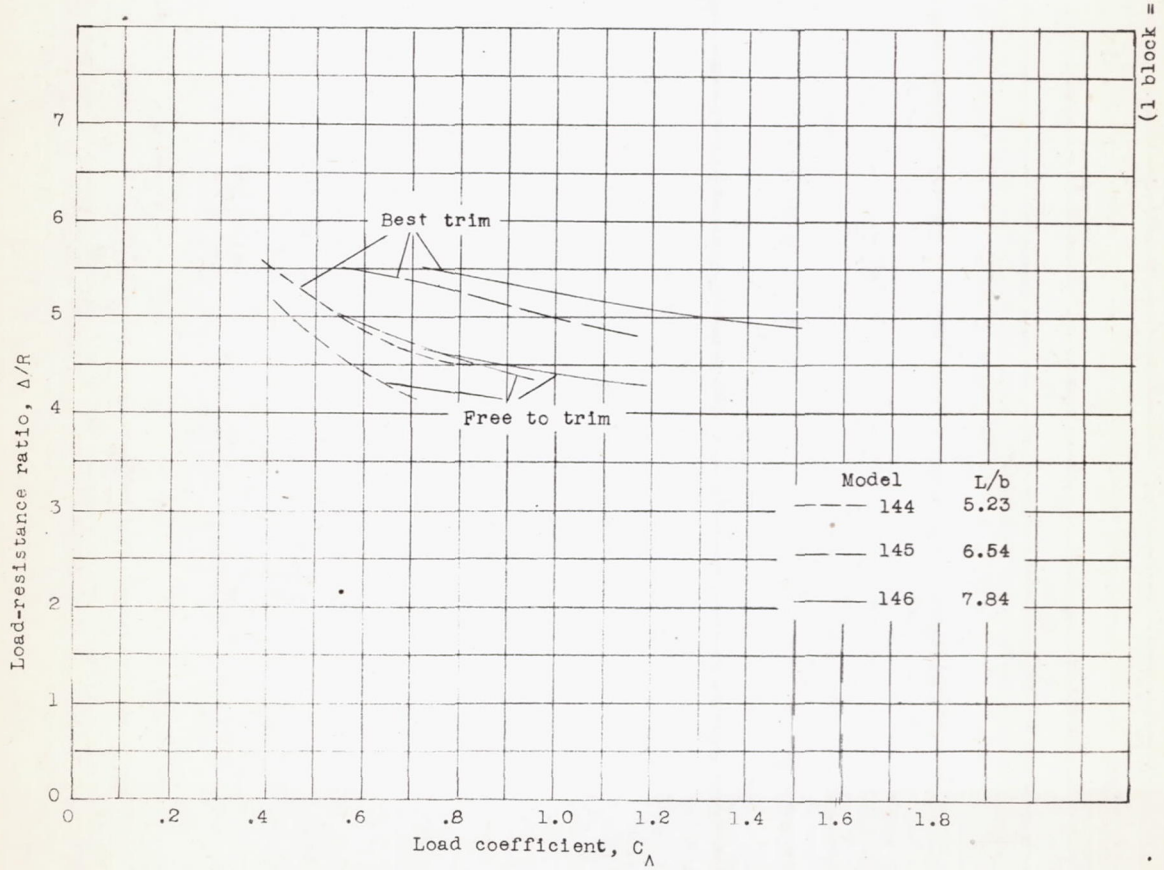

(b) Variation at hump speeds, best trim and free to trim.

Figure 34.- Variation of load-resistance ratio with load coefficient.

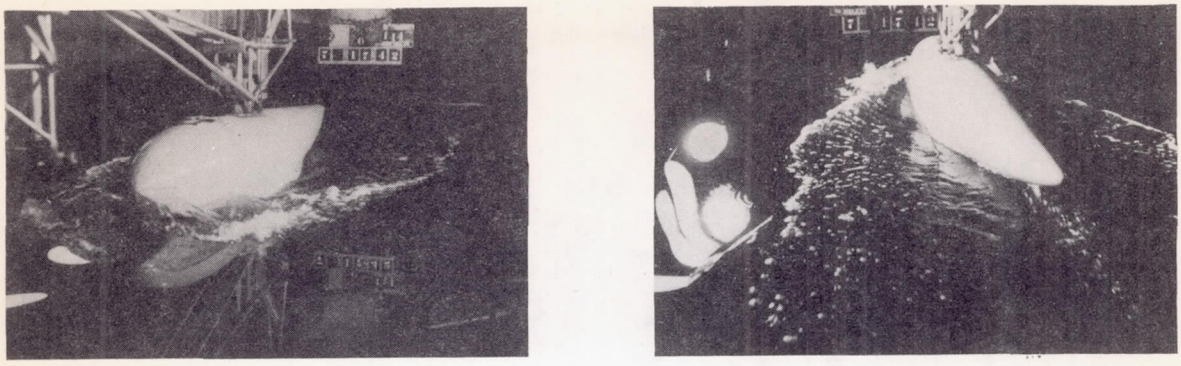

(a) Model 144. Speed, 6.4 feet per second; trim, 2.5°; C_{Δ_o}, 0.67.

(b) Model 145. Speed, 6.2 feet per second; trim, 2.5°; C_{Δ_o}, 0.94.

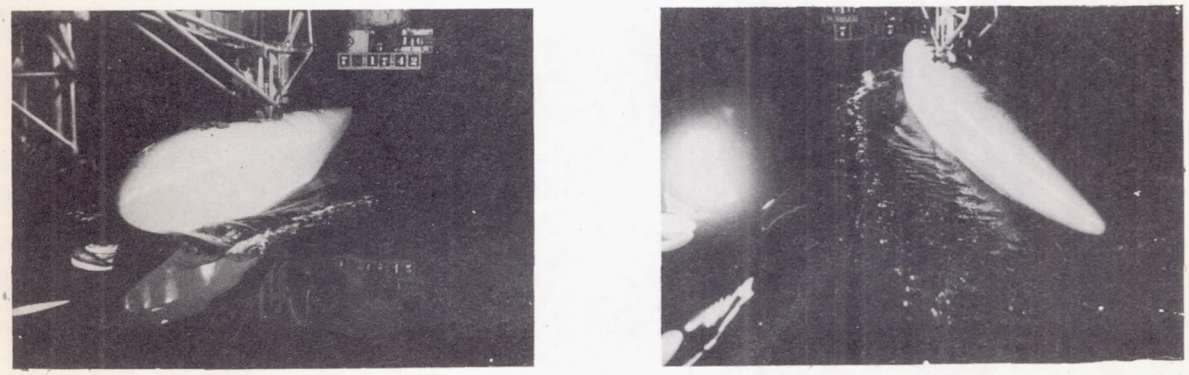

LMAL 34107

(c) Model 146. Speed, 6.0 feet per second; trim, 2.4°; C_{Δ_o}, 1.24.

Figure 35.- Spray photographs, free to trim. Δ_o = 100 pounds.

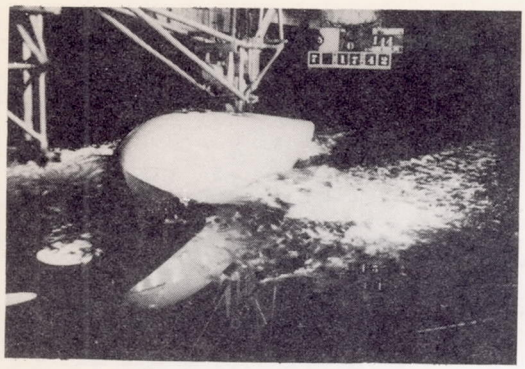

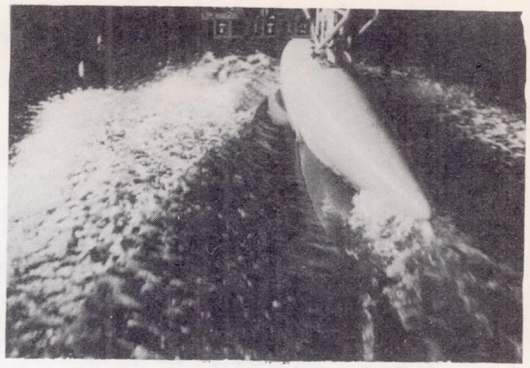

(d) Model 144. Speed, 10.3 feet per second; trim, 5.7°; C_{Δ_o}, 0.67.

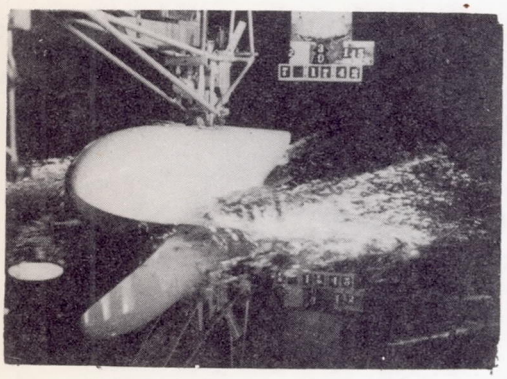

(e) Model 145. Speed, 10.5 feet per second; trim, 5.2°; C_{Δ_o}, 0.94.

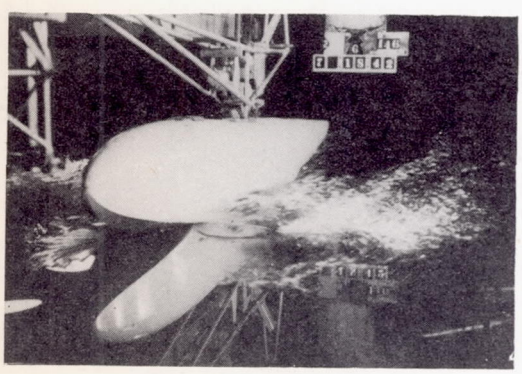

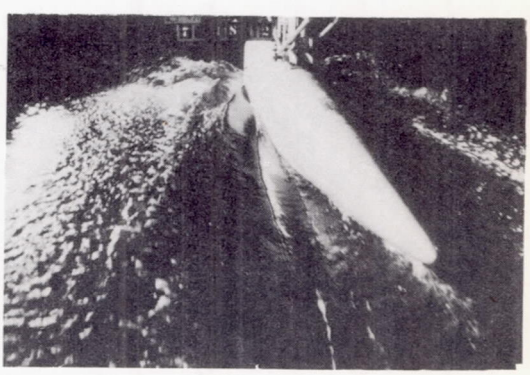

(f) Model 146. Speed, 10.2 feet per second; trim, 4.6°; C_{Δ_o}, 1.24.

LMAL 34108

Figure 35.- Continued. Δ_o = 100 pounds.

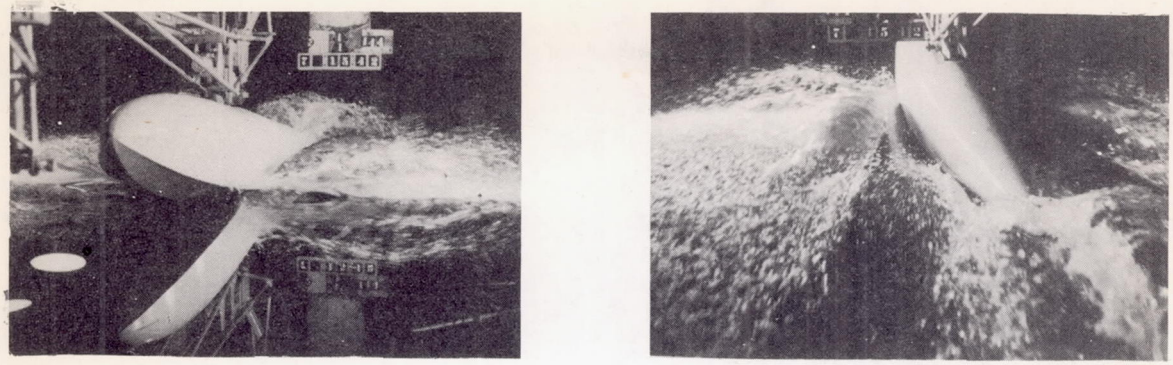

(g) Model 144. Speed, 15.0 feet per second; trim, 9.4°; C_{Δ_o}, 0.67.

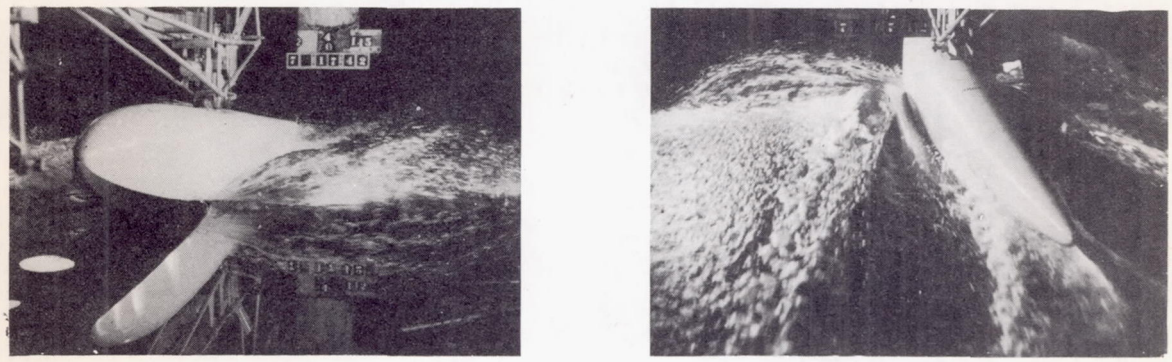

(h) Model 145. Speed, 15.2 feet per second; trim, 6.6°; C_{Δ_o}, 0.94.

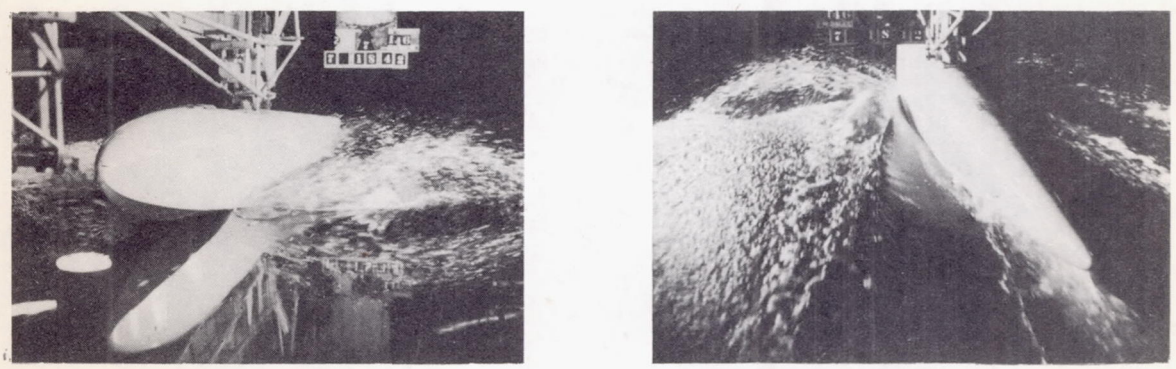

LMAL 34109

(i) Model 146. Speed, 15.0 feet per second; trim, 5.5°; C_{Δ_c}, 1.24.

Figure 35.- Continued. Δ_o = 100 pounds.

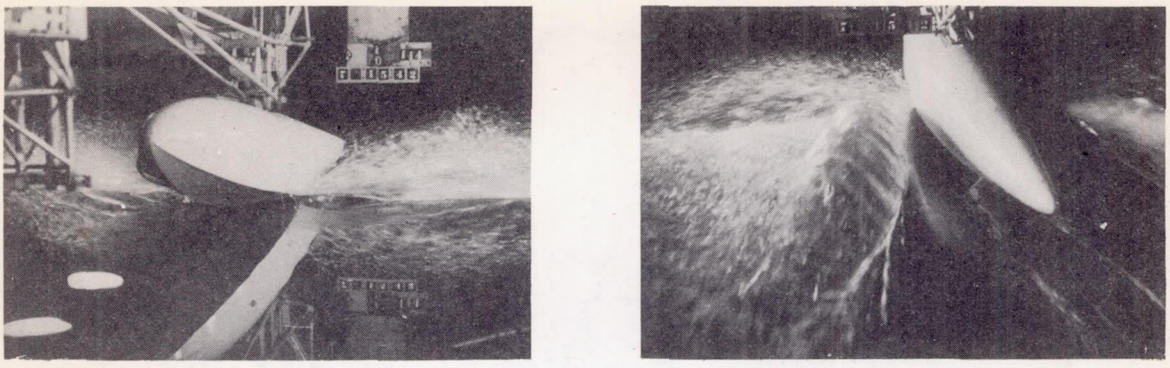

(j) Model 144. Speed, 19.9 feet per second; trim, 9.0°; C_{Δ_o}, 0.67.

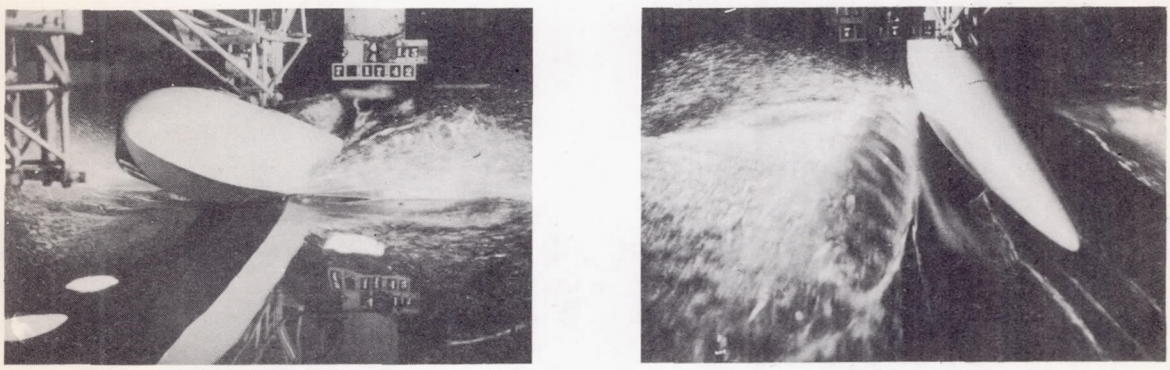

(k) Model 145. Speed, 20.5 feet per second; trim, 9.4°; C_{Δ_o}, 0.94.

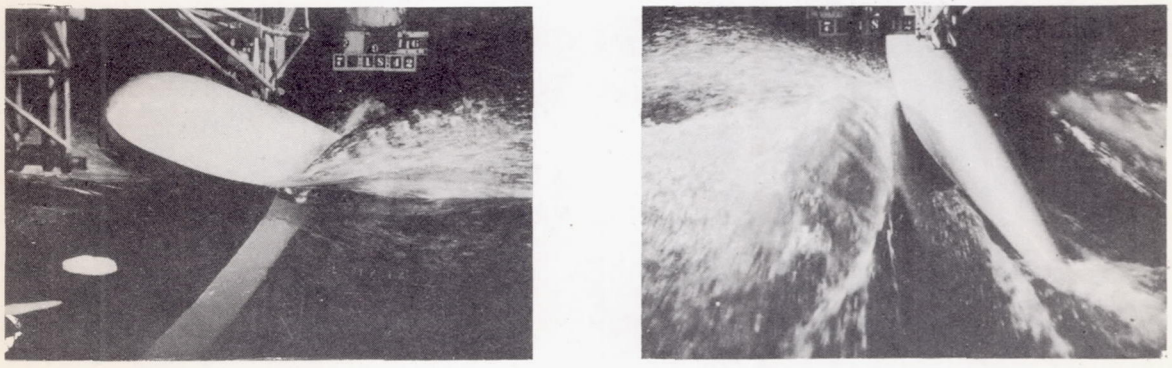

LMAL 34110

(l) Model 146. Speed, 20.4 feet per second; trim, 10.0°; C_{Δ_o}, 1.24.

Figure 35.- Continued. Δ_o = 100 pounds.

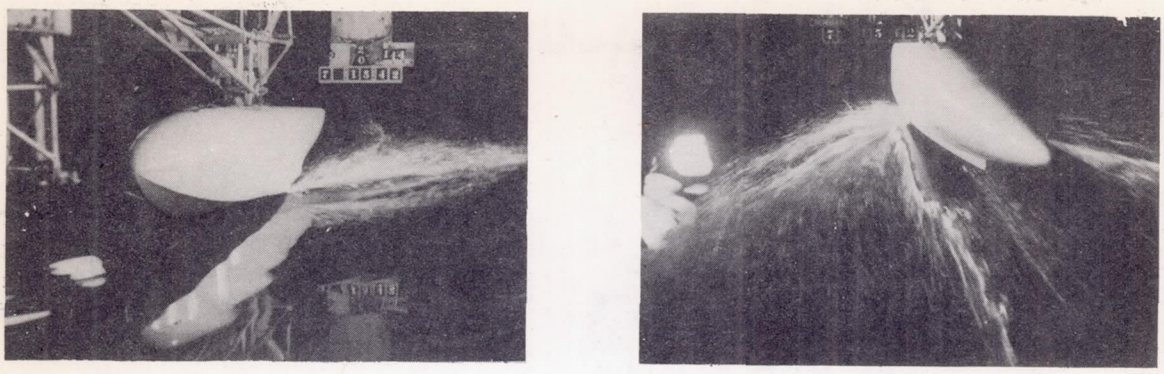

(m) Model 144. Speed, 30.6 feet per second; trim, 3.2°; C_{Δ_o}, 0.67.

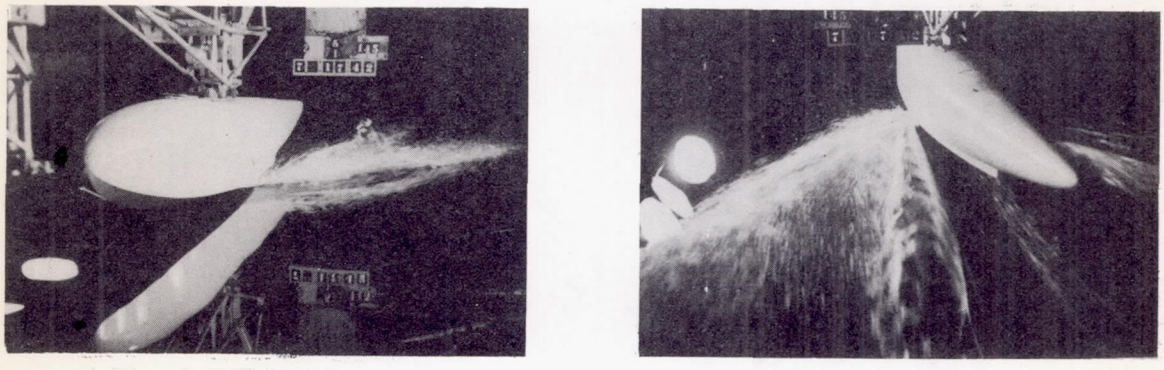

(n) Model 145. Speed, 30.7 feet per second; trim, 3.2°; C_{Δ_o}, 0.94.

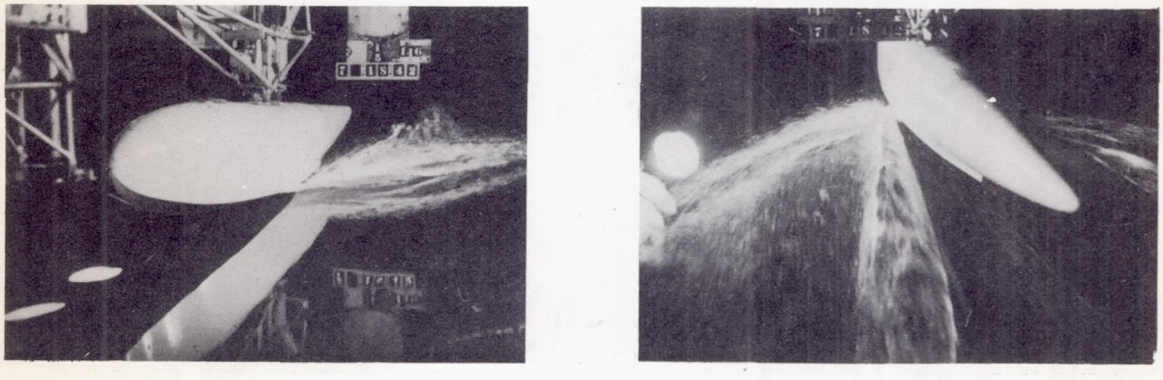

LMAL 3411H

(o) Model 146. Speed, 31.0 feet per second; trim, 3.4°; C_{Δ_o}, 1.24.

Figure 35.- Concluded. Δ_o = 100 pounds.

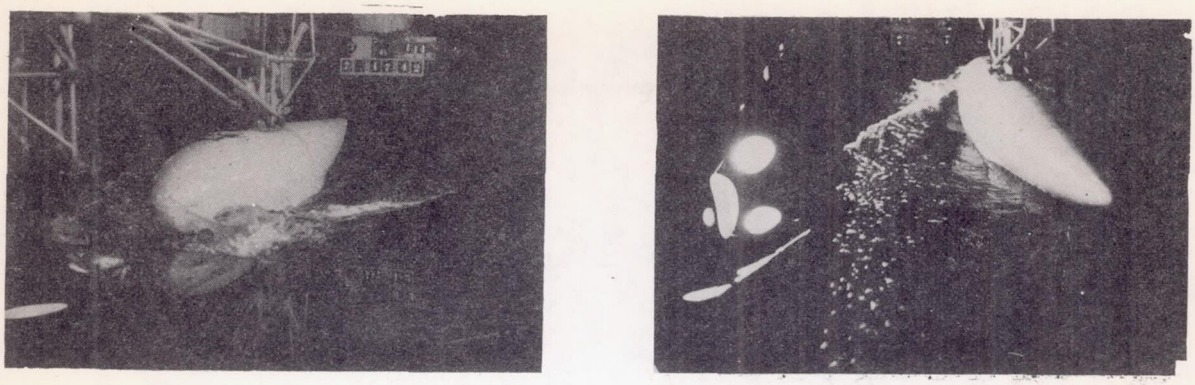

(a) Model 144. Speed, 6.5 feet per second; trim, 2.3°; C_{Δ_o}, 0.81.

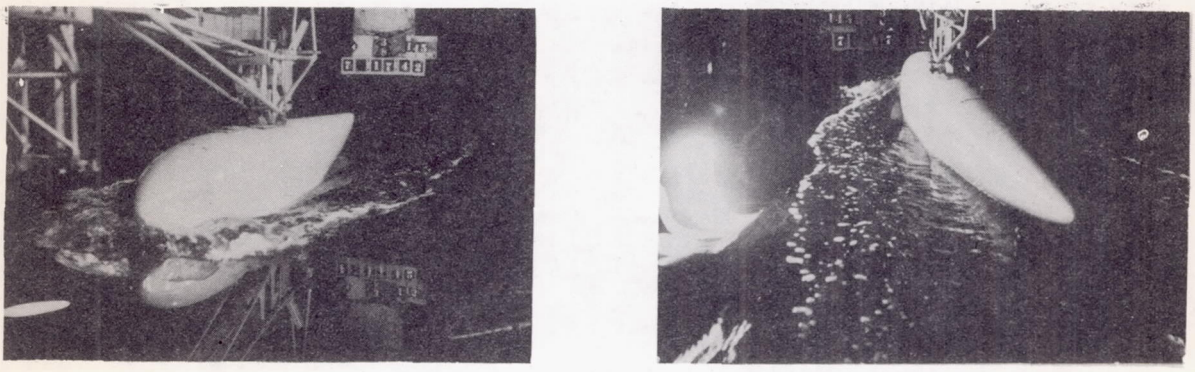

(b) Model 145. Speed, 6.2 feet per second; trim, 2.4°; C_{Δ_o}, 1.13.

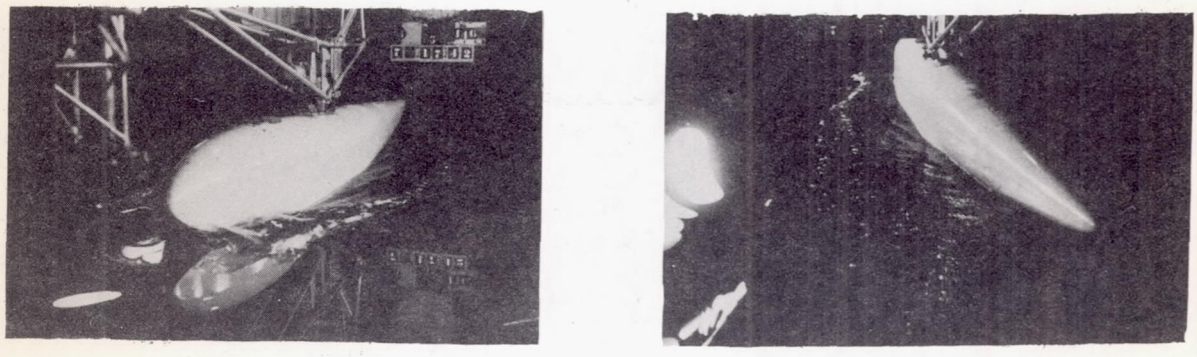

LMAL 34112

(c) Model 146. Speed, 6.0 feet per second; trim, 2.4°; C_{Δ_o}, 1.49.

Figure 36.- Spray photographs, free to trim. Δ_o = 120 pounds.

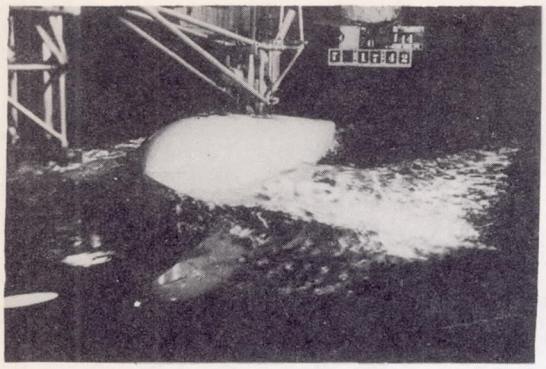

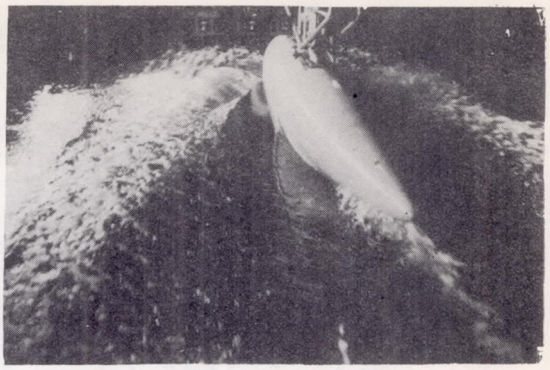

(d) Model 144. Speed, 10.3 feet per second; trim, 5.6°; C_{Δ_o}, 0.81.

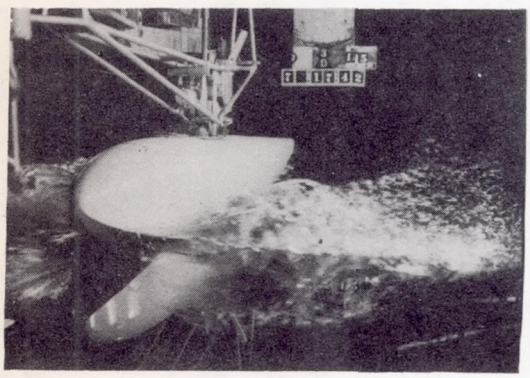

(e) Model 145. Speed, 10.6 feet per second; trim, 5.2°; C_{Δ_o}, 1.13.

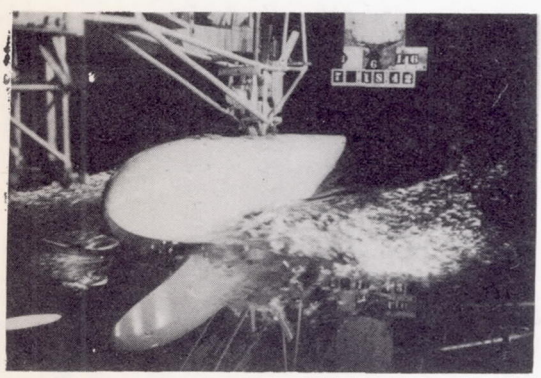

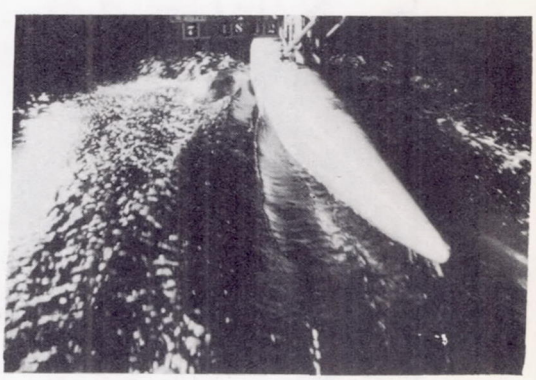

(f) Model 146. Speed, 10.2 feet per second; trim, 4.5°; C_{Δ_o}, 1.49.

LMAL 34113

Figure 36.- Continued. Δ_o = 120 pounds.

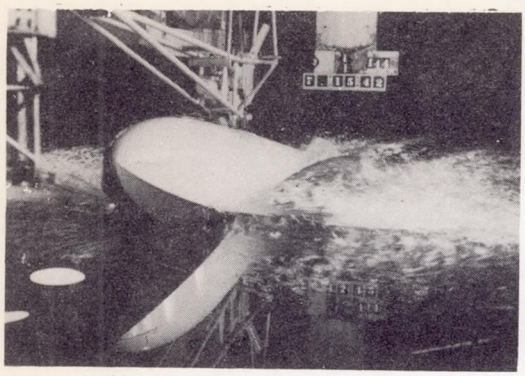

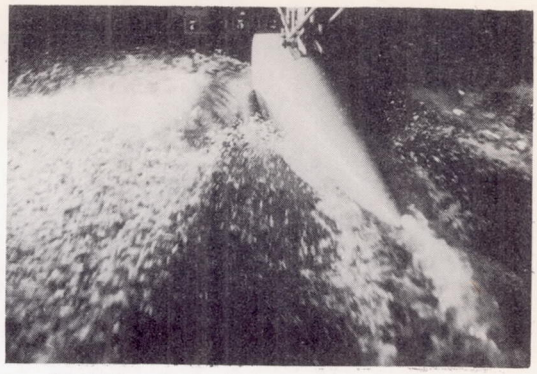

(g) Model 144. Speed, 15.0 feet per second; trim, 8.7°; C_{Δ_o}, 0.81.

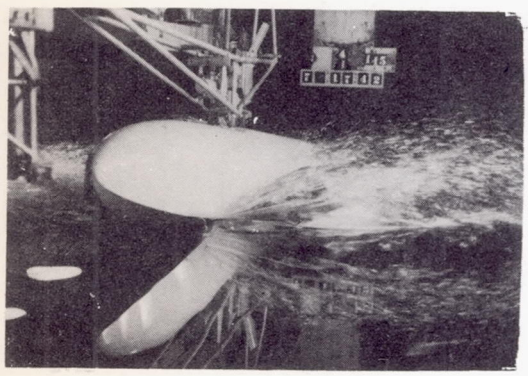

(h) Model 145. Speed, 15.7 feet per second; trim, 6.7°; C_{Δ_o}, 1.13.

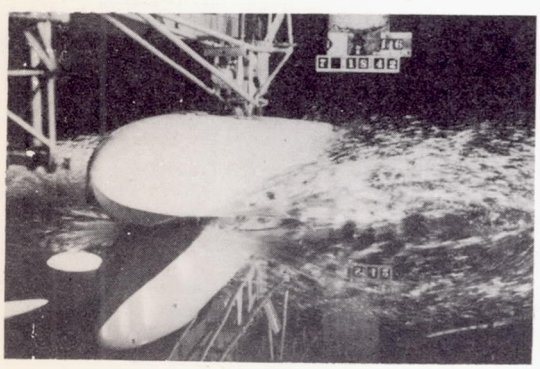

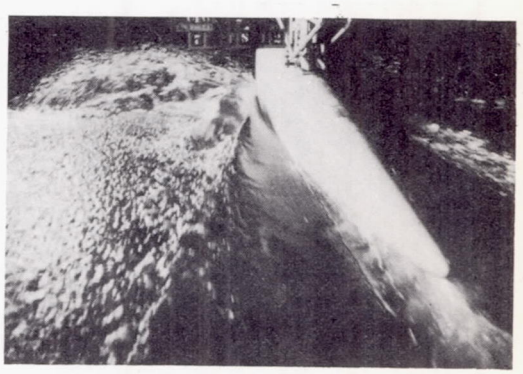

(i) Model 146. Speed, 15.0 feet per second; trim, 5.5°; C_{Δ_o}, 1.49.

LMAL 34114

Figure 36.- Continued. Δ_o = 120 pounds.

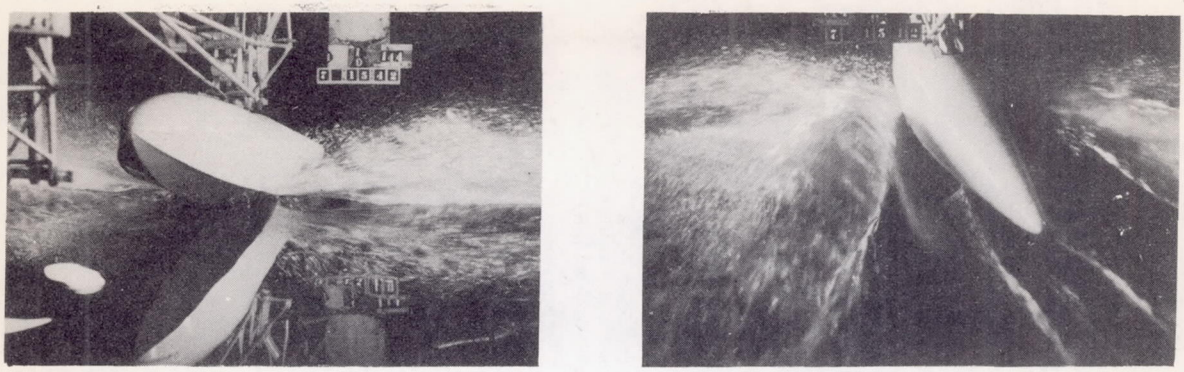

(j) Model 144. Speed, 19.9 feet per second; trim, 10.3°; $C\Delta_o$, 0.81.

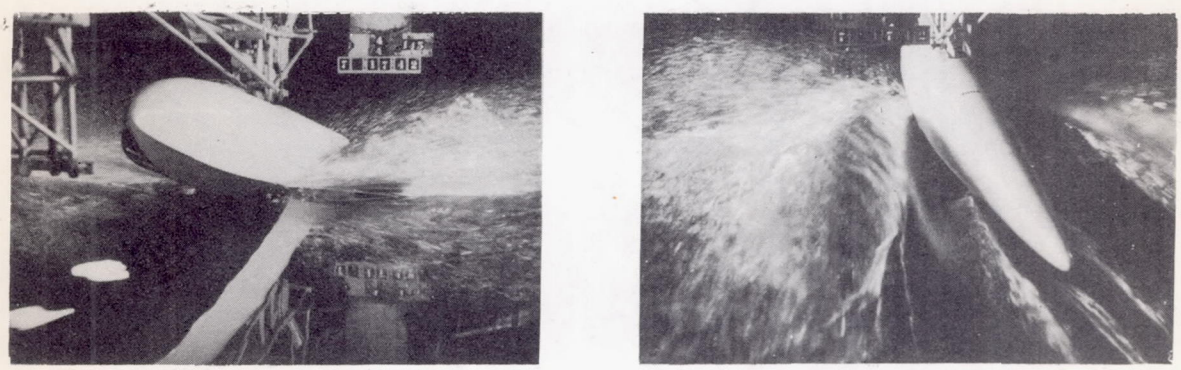

(k) Model 145. Speed, 20.4 feet per second; trim, 10.5°; $C\Delta_o$, 1.13.

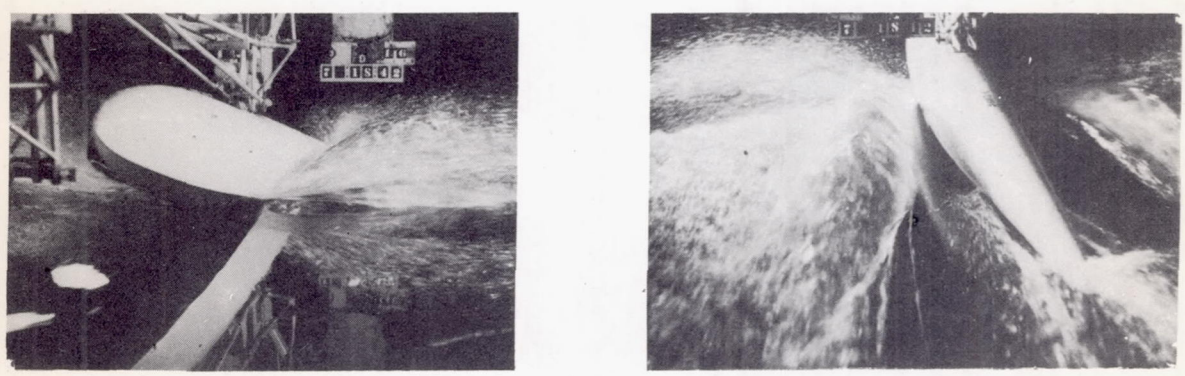

(l) Model 146. Speed, 20.4 feet per second; trim, 9.8°; $C\Delta_o$, 1.49.

LMAL 34115

Figure 36.- Continued. Δ_o = 120 pounds.

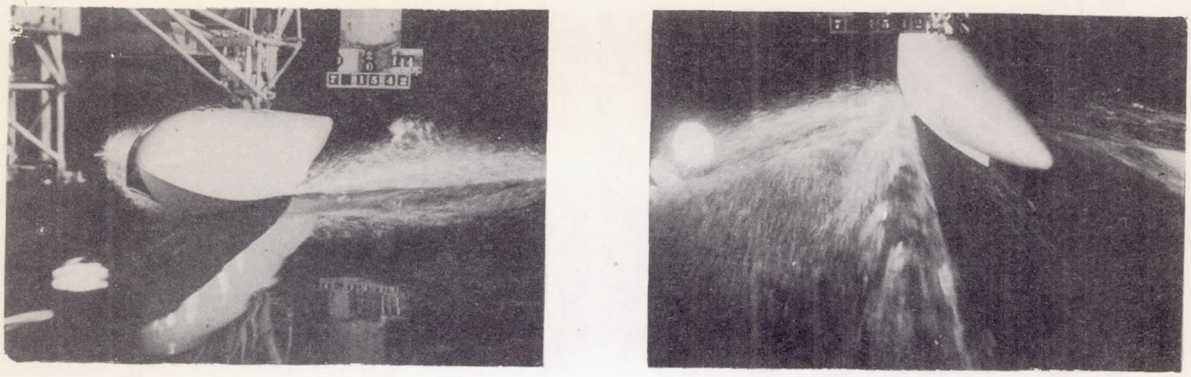

(m) Model 144. Speed, 30.4 feet per second; trim, 4.1°; C_{Δ_o}, 0.81.

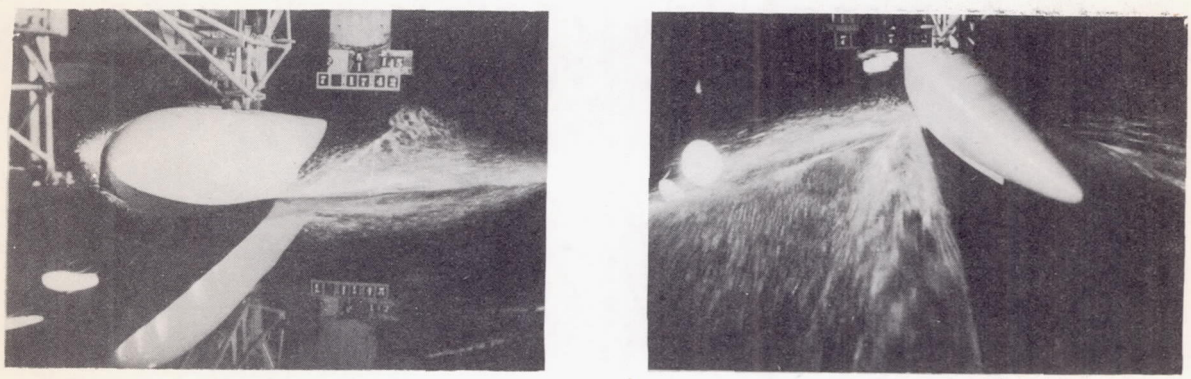

(n) Model 145. Speed, 30.6 feet per second; trim, 4.4°; C_{Δ_o}, 1.13.

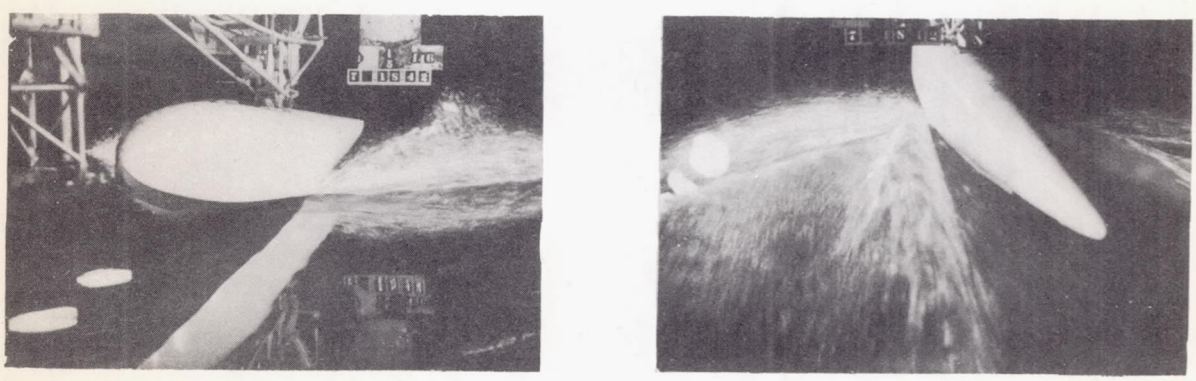

LMAL 34116

(o) Model 146. Speed, 30.8 feet per second; trim, 5.0°; C_{Δ_o}, 1.49.

Figure 36.- Concluded. Δ_o = 120 pounds.

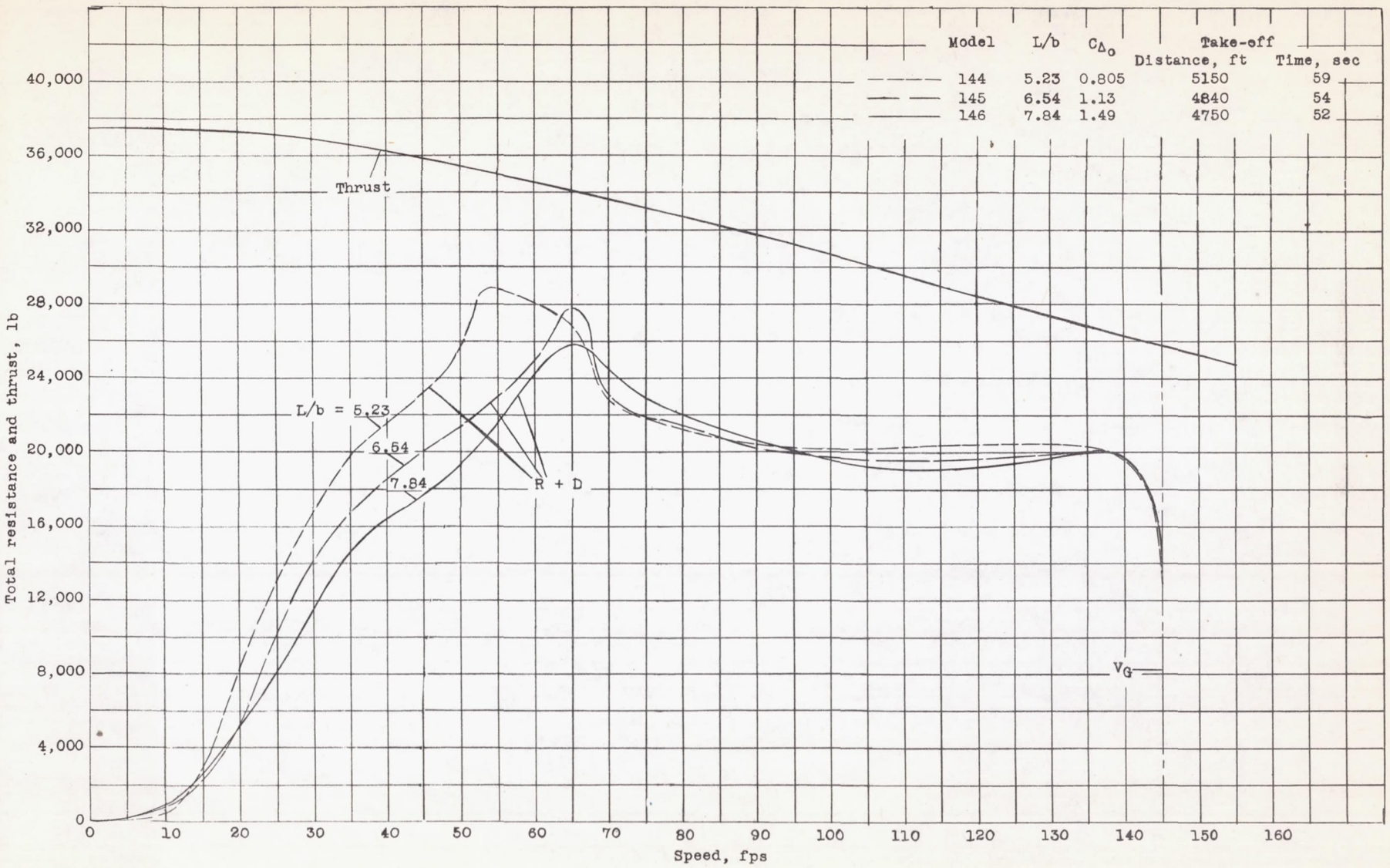

(1 block = 10/40")

Figure 37.- Take-off characteristics of three 140,000-pound flying boats with hull lines of models 144, 145, and 146, assuming hulls 10.5 times size of models.

Fig. 37

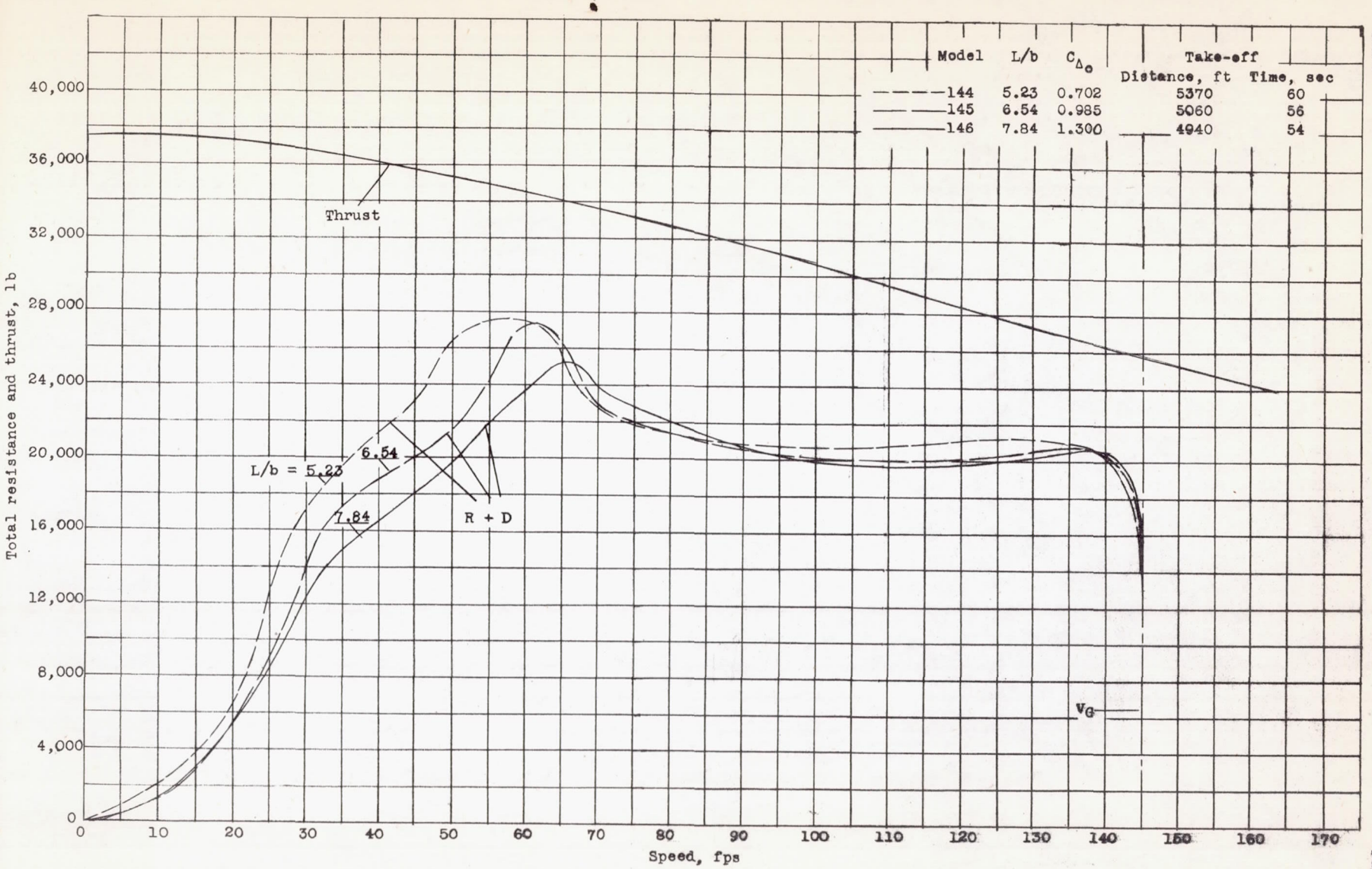

(1 block = 10/40")

Figure 38.- Take-off characteristics of three 140,000-pound flying boats with hull lines of models 144, 145, and 146, assuming hulls 11 times size of models.

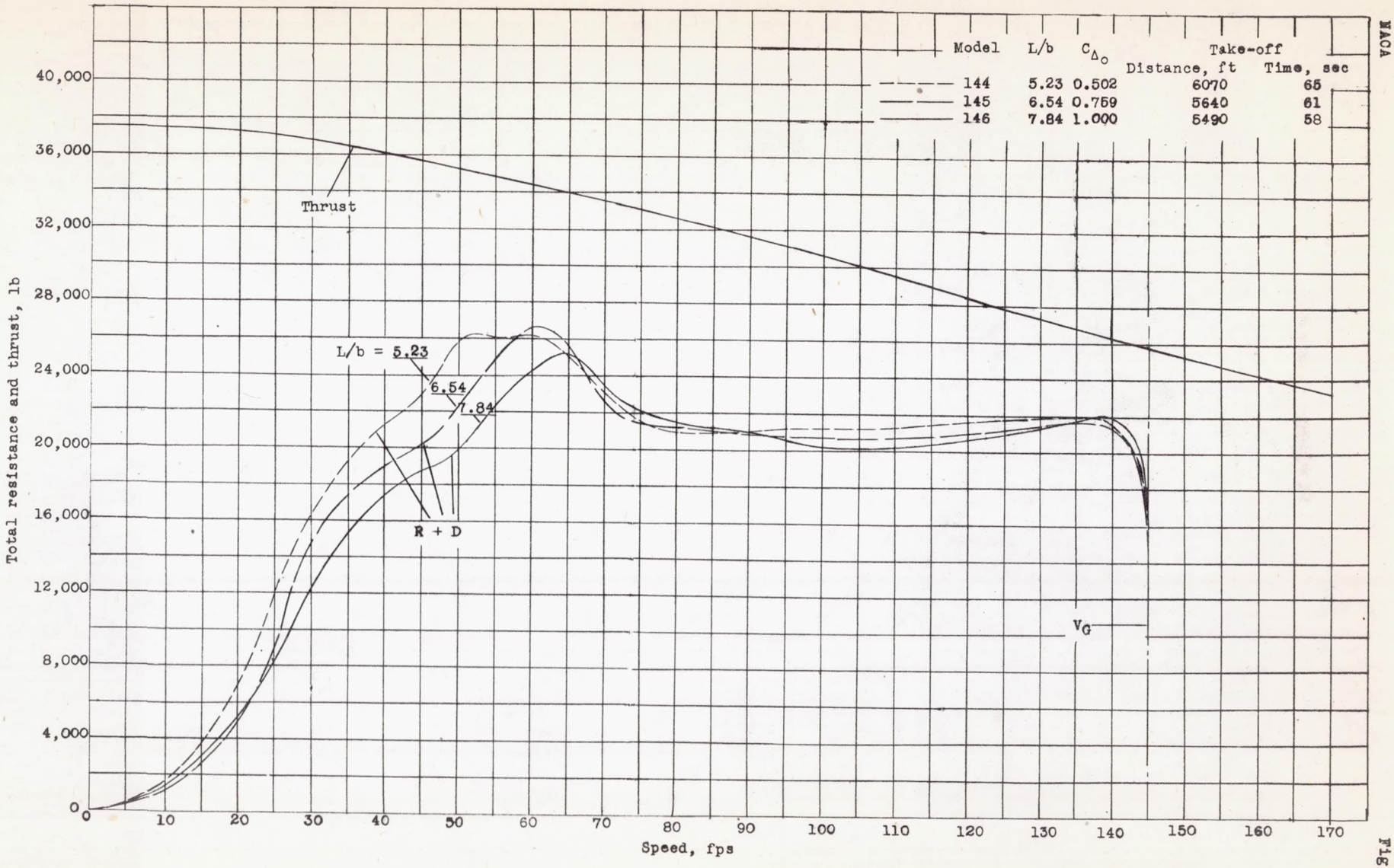

(1 block = 10/40")

Figure 39.- Take-off characteristics of three 140,000-pound flying boats with hull lines of models 144, 145, and 146, assuming hulls 12 times size of models.